38. Cantrell SM, Joy-Schlezinger J, Stegeman JJ, Tillitt DE, Hannink M. Correlation of 2,3,7,8-tetrachlorodibenzo-p-dioxin-induced apoptotic cell death in the embryonic vasculature with embryotoxicity. Toxicol Appl Pharmacol 1998;148:24–34.
39. Christensen JG, Gonzales AJ, Cattley RC, Goldsworthy TL. Regulation of apoptosis in mouse hepatocytes and alteration of apoptosis by nongenotoxic carcinogens. Cell Growth Differ 1998;9:815–25.
40. Kamath AB, Xu H, Nagarkatti PS, Nagarkatti M. Evidence for the induction of apoptosis in thymocytes by 2,3,7,8-tetrachlorodibenzo-p-dioxin in vivo. Toxicol Appl Pharmacol 1997;142:367–77.
41. Kamath AB, Camacho I, Nagarkatti PS, Nagarkatti M. Role of Fas-Fas ligand interactions in 2,3,7,8-tetrachlorodibenzo-p-dioxin (TCDD)-induced immunotoxicity: increased resistance of thymocytes from Fas-deficient (lpr) and Fas ligand-defective (gld) mice to TCDD-induced toxicity. Toxicol Appl Pharmacol 1999;160:141–55.
42. McConkey DJ, Hartzell P, Duddy SK, Hakansson H, Orrenius S. 2,3,7,8-Tetrachlorodibenzo-p-dioxin kills immature thymocytes by Ca2+-mediated endonuclease activation. Science 1988;242:256–9.
43. Rhile MJ, Nagarkatti M, Nagarkatti PS. Role of Fas apoptosis and MHC genes in 2,3,7,8-tetrachlorodibenzo-p-dioxin (TCDD)-induced immunotoxicity of T cells. Toxicology 1996;110:153–67.
44. Sakamoto MK, Mima S, Tanimura TA. Morphological study of liver lesions in Xenopus larvae exposed to 2,3,7,8-tetrachlorodibenzo-p-dioxin (TCDD) with special reference to apoptosis of hepatocytes. J Environ Pathol Toxicol Oncol 1995;14:69–82.
45. Okey AB, Riddick DS, Harper PA. Molecular biology of the aromatic hydrocarbon (dioxin) receptor. Trends Pharmacol Sci 1994;15:226–32.
46. Schmidt JV, Su GH, Reddy JK, Simon MC, Bradfield CA. Characterization of a murine Ahr null allele: involvement of the Ah receptor in hepatic growth and development. Proc Natl Acad Sci U S A 1996;93:6731–6.
47. Park KT, Mitchell KA, Huang G, Elferink CJ. The aryl hydrocarbon receptor predisposes hepatocytes to Fas-mediated apoptosis. Mol Pharmacol 2005;67:612–22.
48. Ziegelbauer J, Shan B, Yager D, Larabell C, Hoffmann B, Tjian R. Transcription factor MIZ-1 is regulated via microtubule association. Mol Cell 2001;8:339–49.
49. Ziegelbauer J, Wei J, Tjian R. Myc-interacting protein 1 target gene profile: a link to microtubules, extracellular signal-regulated kinase, and cell growth. Proc Natl Acad Sci U S A 2004;101:458–63.
50. Lu TT, Makishima M, Repa JJ, Schoonjans K, Kerr TA, Auwerx J, et al. Molecular basis for feedback regulation of bile acid synthesis by nuclear receptors. Mol Cell 2000;6:507–15.
51. Delerive P, Galardi CM, Bisi JE, Nicodeme E, Goodwin B. Identification of liver receptor homolog-1 as a novel regulator of apolipoprotein AI gene transcription. Mol Endocrinol 2004;18:2378–87.
52. Zanjani ED, Poster J, Burlington H, Mann LI, Wasserman LR. Liver as the primary site of erythropoietin formation in the fetus. J Lab Clin Med 1977;89:640–4.
53. Dame C, Fahnenstich H, Freitag P, Hofmann D, Abdul-Nour T, Bartmann P, et al. Erythropoietin mRNA expression in human fetal and neonatal tissue. Blood 1998;92:3218–25.
54. Weiss MJ, Orkin SH. GATA transcription factors: key regulators of hematopoiesis. Exp Hematol 1995;23:99–107.
55. Aird WC, Parvin JD, Sharp PA, Rosenberg RD. The interaction of GATA-binding proteins and basal transcription factors with GATA box-containing core promoters. A model of tissue-specific gene expression. J Biol Chem 1994;269:883–9.
56. Nemer G, Nemer M. Transcriptional activation of BMP-4 and regulation of mammalian organogenesis by GATA-4 and -6. Dev Biol 2003;254:131–48.
57. Cirillo LA, Lin FR, Cuesta I, Friedman D, Jarnik M, Zaret KS. Opening of compacted chromatin by early developmental transcription factors HNF3 (FoxA) and GATA-4. Mol Cell 2002;9:279–89.
58. Goldberg MA, Glass GA, Cunningham JM, Bunn HF. The regulated expression of erythropoietin by two human hepatoma cell lines. Proc Natl Acad Sci U S A 1987;84:7972–6.
59. Dame C, Sola MC, Lim KC, Leach KM, Fandrey J, Ma Y, et al. Hepatic erythropoietin gene regulation by GATA-4. J Biol Chem 2004;279:2955–61.
60. Guo S, Rena G, Cichy S, He X, Cohen P, Unterman T. Phosphorylation of serine 256 by protein kinase B disrupts transactivation by FKHR and mediates effects of insulin on insulin-like growth factor-binding protein-1 promoter activity through a conserved insulin response sequence. J Biol Chem 1999;274:17184–92.
61. Puigserver P, Rhee J, Donovan J, Walkey CJ, Yoon JC, Oriente F, et al. Insulin-regulated hepatic gluconeogenesis through FOXO1-PGC-1alpha interaction. Nature 2003;423:550–5.
62. Schmoll D, Walker KS, Alessi DR, Grempler R, Burchell A, Guo S, et al. Regulation of glucose-6-phosphatase gene expression by protein kinase Balpha and the forkhead transcription factor FKHR. Evidence for insulin response unit-dependent and -independent effects of insulin on promoter activity. J Biol Chem 2000;275:36324–33.
63. Vander Kooi BT, Streeper RS, Svitek CA, Oeser JK, Powell DR, O'Brien RM. The three insulin response sequences in the glucose-6-phosphatase catalytic subunit gene promoter are functionally distinct. J Biol Chem 2003;278:11782–93.
64. Yeagley D, Guo S, Unterman T, Quinn PG. Gene- and activation-specific mechanisms for insulin inhibition of basal and glucocorticoid-induced insulin-like growth factor binding protein-1 and phosphoenolpyruvate carboxykinase transcription. Roles of forkhead and insulin response sequences. J Biol Chem 2001;276:33705–10.
65. Nakae J, Park BC, Accili D. Insulin stimulates phosphorylation of the forkhead transcription factor FKHR on serine 253 through a Wortmannin-sensitive pathway. J Biol Chem 1999;274:15982–5.
66. Rena G, Guo S, Cichy SC, Unterman TG, Cohen P. Phosphorylation of the transcription factor forkhead family member FKHR by protein kinase B. J Biol Chem 1999;274:17179–83.
67. Biggs WH 3rd, Meisenhelder J, Hunter T, Cavenee WK, Arden KC. Protein kinase B/Akt-mediated phosphorylation promotes nuclear exclusion of the winged helix transcription factor FKHR1. Proc Natl Acad Sci U S A 1999;96:7421–6.
68. Matsuzaki H, Daitoku H, Hatta M, Tanaka K, Fukamizu A. Insulin-induced phosphorylation of FKHR (Foxo1) targets to proteasomal degradation. Proc Natl Acad Sci U S A 2003;100:11285–90.
69. Rena G, Prescott AR, Guo S, Cohen P, Unterman TG. Roles of the forkhead in rhabdomyosarcoma (FKHR) phosphorylation sites in regulating 14-3-3 binding, transactivation and nuclear targetting. Biochem J 2001;354:605–12.
70. Zhang X, Gan L, Pan H, Guo S, He X, Olson ST, et al. Phosphorylation of serine 256 suppresses transactivation by

FKHR (FOXO1) by multiple mechanisms. Direct and indirect effects on nuclear/cytoplasmic shuttling and DNA binding. J Biol Chem 2002;277:45276–84.
71. Sotaniemi EA, Pelkonen O, Arranto AJ, Tapanainen P, Rautio A, Pasanen M. Diabetes and elimination of antipyrine in man: an analysis of 298 patients classified by type of diabetes, age, sex, duration of disease and liver involvement. Pharmacol Toxicol 2002;90:155–60.
72. Thummel KE, Schenkman JB. Effects of testosterone and growth hormone treatment on hepatic microsomal P450 expression in the diabetic rat. Mol Pharmacol 1990; 37:119–29.
73. Yamazoe Y, Murayama N, Shimada M, Yamauchi K, Kato R. Cytochrome P450 in livers of diabetic rats: regulation by growth hormone and insulin. Arch Biochem Biophys 1989; 268:567–75.
74. Kawamura A, Yoshida Y, Kimura N, Oda H, Kakinuma A. Phosphorylation/Dephosphorylation steps are crucial for the induction of CYP2B1 and CYP2B2 gene expression by phenobarbital. Biochem Biophys Res Commun 1999;264: 530–6.
75. Sidhu JS, Omiecinski CJ. Insulin-mediated modulation of cytochrome P450 gene induction profiles in primary rat hepatocyte cultures. J Biochem Mol Toxicol 1999;13:1–9.
76. Yoshida Y, Kimura N, Oda H, Kakinuma A. Insulin suppresses the induction of CYP2B1 and CYP2B2 gene expression by phenobarbital in adult rat cultured hepatocytes. Biochem Biophys Res Commun 1996;229:182–8.
77. Honkakoski P, Zelko I, Sueyoshi T, Negishi M. The nuclear orphan receptor CAR-retinoid X receptor heterodimer activates the phenobarbital-responsive enhancer module of the CYP2B gene. Mol Cell Biol 1998;18:5652–8.
78. Wei P, Zhang J, Egan-Hafley M, Liang S, Moore DD. The nuclear receptor CAR mediates specific xenobiotic induction of drug metabolism. Nature 2000;407:920–3.
79. Ueda A, Hamadeh HK, Webb HK, Yamamoto Y, Sueyoshi T, Afshari CA, et al. Diverse roles of the nuclear orphan receptor CAR in regulating hepatic genes in response to phenobarbital. Mol Pharmacol 2002;61:1–6.
80. Kodama S, Koike C, Negishi M, Yamamoto Y. Nuclear receptors CAR and PXR cross talk with FOXO1 to regulate genes that encode drug-metabolizing and gluconeogenic enzymes. Mol Cell Biol 2004;24:7931–40.
81. Brown MS, Goldstein JL. A receptor-mediated pathway for cholesterol homeostasis. Science 1986;232:34–47.
82. Eden ER, Patel DD, Sun XM, Burden JJ, Themis M, Edwards M, et al. Restoration of LDL receptor function in cells from patients with autosomal recessive hypercholesterolemia by retroviral expression of ARH1. J Clin Invest 2002; 110:1695–702.
83. Norman D, Sun XM, Bourbon M, Knight BL, Naoumova RP, Soutar AK. Characterization of a novel cellular defect in patients with phenotypic homozygous familial hypercholesterolemia. J Clin Invest 1999;104:619–28.
84. Wilund KR, Yi M, Campagna F, Arca M, Zuliani G, Fellin R, et al. Molecular mechanisms of autosomal recessive hypercholesterolemia. Hum Mol Genet 2002;11:3019–30.
85. Sirinian MI, Belleudi F, Campagna F, Ceridono M, Garofalo T, Quagliarini F, et al. Adaptor protein ARH is recruited to the plasma membrane by low density lipoprotein (LDL) binding and modulates endocytosis of the LDL/LDL receptor complex in hepatocytes. J Biol Chem 2005;280: 38416–23.
86. Schafer DF, Sorrell MF. Hepatocellular carcinoma. Lancet 1999;353:1253–7.
87. Geller SA. Hepatitis B and hepatitis C. Clin Liver Dis 2002; 6:317–34.
88. Iino S. Natural history of hepatitis B and C virus infections. Oncology 2002;62:18–23.
89. Nakamoto Y, Guidotti LG, Kuhlen CV, Fowler P, Chisari FV. Immune pathogenesis of hepatocellular carcinoma. J Exp Med 1998;188:341–50.
90. Fujii C, Nakamoto Y, Lu P, Tsuneyama K, Popivanova BK, Kaneko S, et al. Aberrant expression of serine/threonine kinase Pim-3 in hepatocellular carcinoma development and its role in the proliferation of human hepatoma cell lines. Int J Cancer 2005;114:209–18.
91. Deneen B, Welford SM, Ho T, Hernandez F, Kurland I, Denny CT. PIM3 proto-oncogene kinase is a common transcriptional target of divergent EWS/ETS oncoproteins. Mol Cell Biol 2003;23:3897–908.
92. Dyson N. The regulation of E2F by pRB-family proteins. Genes Dev 1998;12:2245–62.
93. Phillips AC, Vousden KH. E2F-1 induced apoptosis. Apoptosis 2001;6:173–82.
94. Sola S, Ma X, Castro RE, Kren BT, Steer CJ, Rodrigues CM. Ursodeoxycholic acid modulates E2F-1 and p53 expression through a caspase-independent mechanism in transforming growth factor beta1-induced apoptosis of rat hepatocytes. J Biol Chem 2003;278:48831–8.
95. Fan G, Ma X, Kren BT, Steer CJ. Unbound E2F modulates TGF-beta1-induced apoptosis in HuH-7 cells. J Cell Sci 2002;115:3181–91.
96. Schwarz JK, Bassing CH, Kovesdi I, Datto MB, Blazing M, George S, et al. Expression of the E2F1 transcription factor overcomes type beta transforming growth factor-mediated growth suppression. Proc Natl Acad Sci U S A 1995;92: 483–7.
97. Botla R, Spivey JR, Aguilar H, Bronk SF, Gores GJ. Ursodeoxycholate (UDCA) inhibits the mitochondrial membrane permeability transition induced by glycochenodeoxycholate: a mechanism of UDCA cytoprotection. J Pharmacol Exp Ther 1995;272:930–8.
98. Rodrigues CM, Fan G, Ma X, Kren BT, Steer CJ. A novel role for ursodeoxycholic acid in inhibiting apoptosis by modulating mitochondrial membrane perturbation. J Clin Invest 1998;101:2790–9.
99. Rodrigues CM, Ma X, Linehan-Stieers C, Fan G, Kren BT, Steer CJ. Ursodeoxycholic acid prevents cytochrome c release in apoptosis by inhibiting mitochondrial membrane depolarization and channel formation. Cell Death Differ 1999;6:842–54.
100. Rodrigues CM, Sola S, Sharpe JC, Moura JJ, Steer CJ. Tauroursodeoxycholic acid prevents Bax-induced membrane perturbation and cytochrome C release in isolated mitochondria. Biochemistry 2003;42:3070–80.
101. Tanaka H, Makino Y, Miura T, Hirano F, Okamoto K, Komura K, et al. Ligand-independent activation of the glucocorticoid receptor by ursodeoxycholic acid. Repression of IFN-gamma-induced MHC class II gene expression via a glucocorticoid receptor-dependent pathway. J Immunol 1996;156:1601–8.
102. Miura T, Ouchida R, Yoshikawa N, Okamoto K, Makino Y, Nakamura T, et al. Functional modulation of the glucocorticoid receptor and suppression of NF-kappaB-dependent transcription by ursodeoxycholic acid. J Biol Chem 2001; 276:47371–8.
103. Bailly-Maitre B, de Sousa G, Boulukos K, Gugenheim J, Rahmani R. Dexamethasone inhibits spontaneous apoptosis in primary cultures of human and rat hepatocytes via Bcl-2 and Bcl-xL induction. Cell Death Differ 2001;8:279–88.
104. Yamamoto M, Fukuda K, Miura N, Suzuki R, Kido T, Komatsu Y. Inhibition by dexamethasone of transforming growth factor beta1-induced apoptosis in rat hepatoma cells:

a possible association with Bcl-xL induction. Hepatology 1998;27:959–66.
105. Almeida OF, Conde GL, Crochemore C, Demeneix BA, Fischer D, Hassan AH, et al. Subtle shifts in the ratio between pro- and antiapoptotic molecules after activation of corticosteroid receptors decide neuronal fate. FASEB J 2000;14:779–90.
106. Hassan AH, von Rosenstiel P, Patchev VK, Holsboer F, Almeida OF. Exacerbation of apoptosis in the dentate gyrus of the aged rat by dexamethasone and the protective role of corticosterone. Exp Neurol 1996;140:43–52.
107. Hassan AH, Patchev VK, von Rosenstiel P, Holsboer F, Almeida OF. Plasticity of hippocampal corticosteroid receptors during aging in the rat. FASEB J 1999;13:115–22.
108. McCullers DL, Herman JP. Mineralocorticoid receptors regulate bcl-2 and p53 mRNA expression in hippocampus. Neuroreport 1998;9:3085–9.
109. Nishi M, Ogawa H, Ito T, Matsuda KI, Kawata M. Dynamic changes in subcellular localization of mineralocorticoid receptor in living cells: in comparison with glucocorticoid receptor using dual-color labeling with green fluorescent protein spectral variants. Mol Endocrinol 2001; 15:1077–92.
110. Sola S, Castro RE, Kren BT, Steer CJ, Rodrigues CM. Modulation of nuclear steroid receptors by ursodeoxycholic acid inhibits TGF-beta1-induced E2F-1/p53-mediated apoptosis of rat hepatocytes. Biochemistry 2004;43:8429–38.
111. Schwabe RF, Uchinami H, Qian T, Bennett BL, Lemasters JJ, Brenner DA. Differential requirement for c-Jun NH2-terminal kinase in TNFalpha- and Fas-mediated apoptosis in hepatocytes. FASEB J 2004;18:720–2.
112. Bailly-Maitre B, de Sousa G, Zucchini N, Gugenheim J, Boulukos KE, Rahmani R. Spontaneous apoptosis in primary cultures of human and rat hepatocytes: molecular mechanisms and regulation by dexamethasone. Cell Death Differ 2002;9:945–55.
113. Krueger A, Schmitz I, Baumann S, Krammer PH, Kirchhoff S. Cellular FLICE-inhibitory protein splice variants inhibit different steps of caspase-8 activation at the CD95 death-inducing signaling complex. J Biol Chem 2001;276: 20633–40.
114. Conticello C, Pedini F, Zeuner A, Patti M, Zerilli M, Stassi G, et al. IL-4 protects tumor cells from anti-CD95 and chemotherapeutic agents via up-regulation of antiapoptotic proteins. J Immunol 2004;172:5467–77.
115. Leverkus M, Neumann M, Mengling T, Rauch CT, Brocker EB, Krammer PH, et al. Regulation of tumor necrosis factor-related apoptosis-inducing ligand sensitivity in primary and transformed human keratinocytes. Cancer Res 2000;60:553–9.
116. Okano H, Shiraki K, Inoue H, Kawakita T, Yamanaka T, Deguchi M, et al. Cellular FLICE/caspase-8-inhibitory protein as a principal regulator of cell death and survival in human hepatocellular carcinoma. Lab Invest 2003;83: 1033–43.
117. Oh HY, Namkoong S, Lee SJ, Por E, Kim CK, Billiar TR, et al. Dexamethasone protects primary cultured hepatocytes from death receptor-mediated apoptosis by upregulation of cFLIP. Cell Death Differ 2006;13:512–23.
118. Bhadriraju K, Hansen LK. Extracellular matrix-dependent myosin dynamics during G1-S phase cell cycle progression in hepatocytes. Exp Cell Res 2004;300:259–71.
119. Coutant A, Rescan C, Gilot D, Loyer P, Guguen-Guillouzo C, Baffet G. PI3K-FRAP/mTOR pathway is critical for hepatocyte proliferation whereas MEK/ERK supports both proliferation and survival. Hepatology 2002;36:1079–88.
120. Iijima Y, Laser M, Shiraishi H, Willey CD, Sundaravadivel B, Xu L, et al. c-Raf/MEK/ERK pathway controls protein kinase C-mediated p70S6K activation in adult cardiac muscle cells. J Biol Chem 2002;277:23065–75.
121. Bessard A, Coutant A, Rescan C, Ezan F, Fremin C, Courselaud B, et al. An MLCK-dependent window in late G1 controls S phase entry of proliferating rodent hepatocytes via ERK-p70S6K pathway. Hepatology 2006; 44:152–63.
122. Suzuki YJ, Forman HJ, Sevanian A. Oxidants as stimulators of signal transduction. Free Radic Biol Med 1997;22: 269–85.
123. Carmody RJ, Cotter TG. Signalling apoptosis: a radical approach. Redox Rep 2001;6:77–90.
124. Ueda S, Masutani H, Nakamura H, Tanaka T, Ueno M, Yodoi J. Redox control of cell death. Antioxid Redox Signal 2002;4:405–14.
125. Suzuki YJ. Growth factor signaling for cardioprotection against oxidative stress-induced apoptosis. Antioxid Redox Signal 2003;5:741–9.
126. Matsuzawa A, Ichijo H. Stress-responsive protein kinases in redox-regulated apoptosis signaling. Antioxid Redox Signal 2005;7:472–81.
127. Culmsee C, Mattson MP. p53 in neuronal apoptosis. Biochem Biophys Res Commun 2005;331:761–77.
128. Shiba D, Shimamoto N. Attenuation of endogenous oxidative stress-induced cell death by cytochrome P450 inhibitors in primary cultures of rat hepatocytes. Free Radic Biol Med 1999;27:1019–26.
129. Ishihara Y, Shiba D, Shimamoto N. Primary hepatocyte apoptosis is unlikely to relate to caspase-3 activity under sustained endogenous oxidative stress. Free Radic Res 2005; 39:163–73.
130. Li LY, Luo X, Wang X. Endonuclease G is an apoptotic DNase when released from mitochondria. Nature 2001;412: 95–9.
131. Van Loo G, Schotte P, van Gurp M, Demol H, Hoorelbeke B, Gevaert K, et al. Endonuclease G: a mitochondrial protein released in apoptosis and involved in caspase-independent DNA degradation. Cell Death Differ 2001;8: 1136–42.
132. Ishihara Y, Shimamoto N. Involvement of endonuclease G in nucleosomal DNA fragmentation under sustained endogenous oxidative stress. J Biol Chem 2006;281:6726–33.
133. Ding Y, Le XP, Zhang QX, Du P. Methylation and mutation analysis of p16 gene in gastric cancer. World J Gastroenterol 2003;9:423–6.
134. Okano M, Bell DW, Haber DA, Li E. DNA methyltransferases Dnmt3a and Dnmt3b are essential for de novo methylation and mammalian development. Cell 1999;99: 247–57.
135. Xu J, Fan H, Zhao ZJ, Zhang JQ, Xie W. Identification of potential genes regulated by DNA methyltransferase 3B in a hepatocellular carcinoma cell line by RNA interference and microarray analysis. Yi Chuan Xue Bao 2005;32:1115–27.
136. Yin M, Wheeler MD, Kono H, Bradford BU, Gallucci RM, Luster MI, et al. Essential role of tumor necrosis factor alpha in alcohol-induced liver injury in mice. Gastroenterology 1999;117:942–52.
137. Bradham CA, Plumpe J, Manns MP, Brenner DA, Trautwein C. Mechanisms of hepatic toxicity. I. TNF-induced liver injury. Am J Physiol 1998;275:G387–92.
138. Slomiany BL, Piotrowski J, Slomiany A. Chronic alcohol ingestion enhances tumor necrosis factor-alpha expression and salivary gland apoptosis. Alcohol Clin Exp Res 1997;21: 1530–3.

139. Lin HZ, Yang SQ, Zeldin G, Diehl AM. Chronic ethanol consumption induces the production of tumor necrosis factor-alpha and related cytokines in liver and adipose tissue. Alcohol Clin Exp Res 1998;22:231S–7S.
140. Deaciuc IV, D'Souza NB, Spitzer JJ. Tumor necrosis factor-alpha cell-surface receptors of liver parenchymal and non-parenchymal cells during acute and chronic alcohol administration to rats. Alcohol Clin Exp Res 1995;19:332–8.
141. Pastorino JG, Hoek JB. Ethanol potentiates tumor necrosis factor-alpha cytotoxicity in hepatoma cells and primary rat hepatocytes by promoting induction of the mitochondrial permeability transition. Hepatology 2000;31:1141–52.
142. Fernandez-Checa JC, Kaplowitz N, Garcia-Ruiz C, Colell A, Miranda M, Mari M, et al. GSH transport in mitochondria: defense against TNF-induced oxidative stress and alcohol-induced defect. Am J Physiol 1997;273:G7–17.
143. Hatano E, Brenner DA. Akt protects mouse hepatocytes from TNF-alpha- and Fas-mediated apoptosis through NK-kappa B activation. Am J Physiol Gastrointest Liver Physiol 2001;281:G1357–68.
144. Kennedy SG, Kandel ES, Cross TK, Hay N. Akt/Protein kinase B inhibits cell death by preventing the release of cytochrome c from mitochondria. Mol Cell Biol 1999;19: 5800–10.
145. Khwaja A. Akt is more than just a Bad kinase. Nature 1999; 401:33–4.
146. Pastorino JG, Shulga N, Hoek JB. TNF-alpha-induced cell death in ethanol-exposed cells depends on p38 MAPK signaling but is independent of Bid and caspase-8. Am J Physiol Gastrointest Liver Physiol 2003;285:G503–16.
147. Shulga N, Hoek JB, Pastorino JG. Elevated PTEN levels account for the increased sensitivity of ethanol-exposed cells to tumor necrosis factor-induced cytotoxicity. J Biol Chem 2005;280:9416–24.
148. Akira S, Hemmi H. Recognition of pathogen-associated molecular patterns by TLR family. Immunol Lett 2003;85: 85–95.
149. Alexopoulou L, Holt AC, Medzhitov R, Flavell RA. Recognition of double-stranded RNA and activation of NF-kappaB by Toll-like receptor 3. Nature 2001;413:732–8.
150. Hoebe K, Du X, Georgel P, Janssen E, Tabeta K, Kim SO, et al. Identification of Lps2 as a key transducer of MyD88-independent TIR signalling. Nature 2003;424:743–8.
151. Oshiumi H, Matsumoto M, Funami K, Akazawa T, Seya T. TICAM-1, an adaptor molecule that participates in Toll-like receptor 3-mediated interferon-beta induction. Nat Immunol 2003;4:161–7.
152. Yamamoto M, Sato S, Mori K, Hoshino K, Takeuchi O, Takeda K, et al. Cutting edge: a novel Toll/IL-1 receptor domain-containing adapter that preferentially activates the IFN-beta promoter in the Toll-like receptor signaling. J Immunol 2002;169:6668–72.
153. Yamamoto M, Sato S, Hemmi H, Hoshino K, Kaisho T, Sanjo H, et al. Role of adaptor TRIF in the MyD88-independent toll-like receptor signaling pathway. Science 2003;301:640–3.
154. Lund JM, Alexopoulou L, Sato A, Karow M, Adams NC, Gale NW, et al. Recognition of single-stranded RNA viruses by Toll-like receptor 7. Proc Natl Acad Sci U S A 2004;101: 5598–603.
155. Honda K, Sakaguchi S, Nakajima C, Watanabe A, Yanai H, Matsumoto M, et al. Selective contribution of IFN-alpha/beta signaling to the maturation of dendritic cells induced by double-stranded RNA or viral infection. Proc Natl Acad Sci U S A 2003;100:10872–7.
156. Edelmann KH, Richardson-Burns S, Alexopoulou L, Tyler KL, Flavell RA, Oldstone MB. Does Toll-like receptor 3 play a biological role in virus infections? Virology 2004;322: 231–8.
157. Yoneyama M, Kikuchi M, Natsukawa T, Shinobu N, Imaizumi T, Miyagishi M, et al. The RNA helicase RIG-I has an essential function in double-stranded RNA-induced innate antiviral responses. Nat Immunol 2004;5:730–7.
158. Li K, Chen Z, Kato N, Gale M Jr, Lemon SM. Distinct poly(I-C) and virus-activated signaling pathways leading to interferon-beta production in hepatocytes. J Biol Chem 2005;280:16739–47.
159. Noguchi M, Hirohashi S. Cell lines from non-neoplastic liver and hepatocellular carcinoma tissue from a single patient. In Vitro Cell Dev Biol Anim 1996;32:135–7.
160. Ikeda M, Sugiyama K, Mizutani T, Tanaka T, Tanaka K, Sekihara H, et al. Human hepatocyte clonal cell lines that support persistent replication of hepatitis C virus. Virus Res 1998;56:157–67.
161. Arima N, Kao CY, Licht T, Padmanabhan R, Sasaguri Y, Padmanabhan R. Modulation of cell growth by the hepatitis C virus nonstructural protein NS5A. J Biol Chem 2001;276: 12675–84.
162. Kato N. Molecular virology of hepatitis C virus. Acta Med Okayama 2001;55:133–59.
163. Ray RB, Ray R. Hepatitis C virus core protein: intriguing properties and functional relevance. FEMS Microbiol Lett 2001;202:149–56.
164. Reed KE, Rice CM. Overview of hepatitis C virus genome structure, polyprotein processing, and protein properties. Curr Top Microbiol Immunol 2000;242:55–84.
165. Dubourdeau M, Miyamura T, Matsuura Y, Alric L, Pipy B, Rousseau D. Infection of HepG2 cells with recombinant adenovirus encoding the HCV core protein induces p21(WAF1) down-regulation—effect of transforming growth factor beta. J Hepatol 2002;37:486–92.
166. Jung EY, Lee MN, Yang HY, Yu D, Jang KL. The repressive activity of hepatitis C virus core protein on the transcription of p21(waf1) is regulated by protein kinase A-mediated phosphorylation. Virus Res 2001;79:109–15.
167. Lu W, Lo SY, Chen M, Wu K, Fung YK, Ou JH. Activation of p53 tumor suppressor by hepatitis C virus core protein. Virology 1999;264:134–41.
168. Marusawa H, Hijikata M, Chiba T, Shimotohno K. Hepatitis C virus core protein inhibits Fas- and tumor necrosis factor alpha-mediated apoptosis via NF-kappaB activation. J Virol 1999;73:4713–20.
169. Ray RB, Steele R, Meyer K, Ray R. Hepatitis C virus core protein represses p21WAF1/Cip1/Sid1 promoter activity. Gene 1998;208:331–6.
170. Scholle F, Li K, Bodola F, Ikeda M, Luxon BA, Lemon SM. Virus-host cell interactions during hepatitis C virus RNA replication: impact of polyprotein expression on the cellular transcriptome and cell cycle association with viral RNA synthesis. J Virol 2004;78:1513–24.
171. Tsuchihara K, Hijikata M, Fukuda K, Kuroki T, Yamamoto N, Shimotohno K. Hepatitis C virus core protein regulates cell growth and signal transduction pathway transmitting growth stimuli. Virology 1999;258:100–7.
172. Dansako H, Naganuma A, Nakamura T, Ikeda F, Nozaki A, Kato N. Differential activation of interferon-inducible genes by hepatitis C virus core protein mediated by the interferon stimulated response element. Virus Res 2003;97:17–30.
173. Naganuma A, Nozaki A, Tanaka T, Sugiyama K, Takagi H, Mori M, et al. Activation of the interferon-inducible 2′-5′-oligoadenylate synthetase gene by hepatitis C virus core protein. J Virol 2000;74:8744–50.

174. Naganuma A, Dansako H, Nakamura T, Nozaki A, Kato N. Promotion of microsatellite instability by hepatitis C virus core protein in human non-neoplastic hepatocyte cells. Cancer Res 2004;64:1307–14.
175. Naka K, Dansako H, Kobayashi N, Ikeda M, Kato N. Hepatitis C virus NS5B delays cell cycle progression by inducing interferon-beta via Toll-like receptor 3 signaling pathway without replicating viral genomes. Virology 2006; 346:348–62.
176. MacDonald G, Shi L, Vande Velde C, Lieberman J, Greenberg AH. Mitochondria-dependent and -independent regulation of Granzyme B-induced apoptosis. J Exp Med 1999; 189:131–44.
177. Song E, Chen J, Su F, Wang M, Heemann U. Granzyme B inhibitor I reduces apoptotic cell death of allogeneic-transplanted hepatocytes in spleen. Transplant Proc 2001; 33:3274–5.
178. Wang J, Li W, Min J, Ou Q, Chen J. Fas siRNA reduces apoptotic cell death of allogeneic-transplanted hepatocytes in mouse spleen. Transplant Proc 2003;35:1594–5.
179. Kondo T, Suda T, Fukuyama H, Adachi M, Nagata S. Essential roles of the Fas ligand in the development of hepatitis. Nat Med 1997;3:409–13.
180. Kuhnel F, Zender L, Paul Y, Tietze MK, Trautwein C, Manns M, et al. NFkappaB mediates apoptosis through transcriptional activation of Fas (CD95) in adenoviral hepatitis. J Biol Chem 2000;275:6421–7.
181. Mundt B, Kuhnel F, Zender L, Paul Y, Tillmann H, Trautwein C, et al. Involvement of TRAIL and its receptors in viral hepatitis. FASEB J 2003;17:94–6.
182. Shi Y. Mechanisms of caspase activation and inhibition during apoptosis. Mol Cell 2002;9:459–70.
183. Nishimura Y, Hirabayashi Y, Matsuzaki Y, Musette P, Ishii A, Nakauchi H, et al. In vivo analysis of Fas antigen-mediated apoptosis: effects of agonistic anti-mouse Fas mAb on thymus, spleen and liver. Int Immunol 1997;9:307–16.
184. Zender L, Hutker S, Liedtke C, Tillmann HL, Zender S, Mundt B, et al. Caspase 8 small interfering RNA prevents acute liver failure in mice. Proc Natl Acad Sci U S A 2003; 100:7797–802.
185. Kanzler S, Galle PR. Apoptosis and the liver. Semin Cancer Biol 2000;10:173–84.
186. Eichhorst ST. Modulation of apoptosis as a target for liver disease. Expert Opin Ther Targets 2005;9:83–99.
187. Gressner AM, Weiskirchen R. The tightrope of therapeutic suppression of active transforming growth factor-beta: high enough to fall deeply? J Hepatol 2003;39:856–9.
188. Mizuguchi Y, Yokomuro S, Mishima T, Arima Y, Shimizu T, Kawahigashi Y, et al. Short hairpin RNA modulates transforming growth factor beta signaling in life-threatening liver failure in mice. Gastroenterology 2005;129:1654–62.
189. Rust C, Gores GJ. Apoptosis and liver disease. Am J Med 2000;108:567–74.
190. Siegel RM, Fleisher TA. The role of Fas and related death receptors in autoimmune and other disease states. J Allergy Clin Immunol 1999;103:729–38.
191. Canbay A, Higuchi H, Bronk SF, Taniai M, Sebo TJ, Gores GJ. Fas enhances fibrogenesis in the bile duct ligated mouse: a link between apoptosis and fibrosis. Gastroenterology 2002;123:1323–30.
192. Galle PR, Hofmann WJ, Walczak H, Schaller H, Otto G, Stremmel W, et al. Involvement of the CD95 (APO-1/Fas) receptor and ligand in liver damage. J Exp Med 1995;182: 1223–30.
193. Li XK, Fujino M, Sugioka A, Morita M, Okuyama T, Guo L, et al. Fulminant hepatitis by Fas-ligand expression in MRL-lpr/lpr mice grafted with Fas-positive livers and wild-type mice with Fas-mutant livers. Transplantation 2001;71: 503–8.
194. Song E, Lee SK, Wang J, Ince N, Ouyang N, Min J, et al. RNA interference targeting Fas protects mice from fulminant hepatitis. Nat Med 2003;9:347–51.
195. Bartenschlager R, Frese M, Pietschmann T. Novel insights into hepatitis C virus replication and persistence. Adv Virus Res 2004;63:71–180.
196. Randall G, Rice CM. Hepatitis C virus cell culture replication systems: their potential use for the development of antiviral therapies. Curr Opin Infect Dis 2001;14: 743–7.
197. Zeuzem S, Feinman SV, Rasenack J, Heathcote EJ, Lai MY, Gane E, et al. Peginterferon alfa-2a in patients with chronic hepatitis C. N Engl J Med 2000;343:1666–72.
198. Heathcote EJ, Shiffman ML, Cooksley WG, Dusheiko GM, Lee SS, Balart L, et al. Peginterferon alfa-2a in patients with chronic hepatitis C and cirrhosis. N Engl J Med 2000;343: 1673–80.
199. Kato N, Hijikata M, Ootsuyama Y, Nakagawa M, Ohkoshi S, Sugimura T, et al. Molecular cloning of the human hepatitis C virus genome from Japanese patients with non-A, non-B hepatitis. Proc Natl Acad Sci U S A 1990;87:9524–8.
200. Bartenschlager R, Lohmann V. Replication of hepatitis C virus. J Gen Virol 2000;81:1631–48.
201. Thomas DL. Hepatitis C epidemiology. Curr Top Microbiol Immunol 2000;242:25–41.
202. McHutchison JG, Patel K. Future therapy of hepatitis C. Hepatology 2002;36:S245–52.
203. Kim WR. The burden of hepatitis C in the United States. Hepatology 2002;36:S30–4.
204. McHutchison JG. Hepatitis C advances in antiviral therapy: what is accepted treatment now? J Gastroenterol Hepatol 2002;17:431–41.
205. McCaffrey AP, Meuse L, Pham TT, Conklin DS, Hannon GJ, Kay MA. RNA interference in adult mice. Nature 2002; 418:38–9.
206. Wilson JA, Jayasena S, Khvorova A, Sabatinos S, Rodrigue-Gervais IG, Arya S, et al. RNA interference blocks gene expression and RNA synthesis from hepatitis C replicons propagated in human liver cells. Proc Natl Acad Sci U S A 2003;100:2783–8.
207. Wilson JA, Richardson CD. Hepatitis C virus replicons escape RNA interference induced by a short interfering RNA directed against the NS5b coding region. J Virol 2005; 79:7050–8.
208. Kapadia SB, Brideau-Andersen A, Chisari FV. Interference of hepatitis C virus RNA replication by short interfering RNAs. Proc Natl Acad Sci U S A 2003;100:2014–8.
209. Randall G, Grakoui A, Rice CM. Clearance of replicating hepatitis C virus replicon RNAs in cell culture by small interfering RNAs. Proc Natl Acad Sci U S A 2003;100:235–40.
210. Blight KJ, McKeating JA, Rice CM. Highly permissive cell lines for subgenomic and genomic hepatitis C virus RNA replication. J Virol 2002;76:13001–14.
211. Choo QL, Richman KH, Han JH, Berger K, Lee C, Dong C, et al. Genetic organization and diversity of the hepatitis C virus. Proc Natl Acad Sci U S A 1991;88:2451–5.
212. Okamoto H, Okada S, Sugiyama Y, Kurai K, Iizuka H, Machida A, et al. Nucleotide sequence of the genomic RNA of hepatitis C virus isolated from a human carrier: comparison with reported isolates for conserved and divergent regions. J Gen Virol 1991;72:2697–704.
213. Yokota T, Sakamoto N, Enomoto N, Tanabe Y, Miyagishi M, Maekawa S, et al. Inhibition of intracellular hepatitis C

virus replication by synthetic and vector-derived small interfering RNAs. EMBO Rep 2003;4:602–8.
214. Kronke J, Kittler R, Buchholz F, Windisch MP, Pietschmann T, Bartenschlager R, et al. Alternative approaches for efficient inhibition of hepatitis C virus RNA replication by small interfering RNAs. J Virol 2004;78:3436–46.
215. Takigawa Y, Nagano-Fujii M, Deng L, Hidajat R, Tanaka M, Mizuta H, et al. Suppression of hepatitis C virus replicon by RNA interference directed against the NS3 and NS5B regions of the viral genome. Microbiol Immunol 2004;48: 591–8.
216. Kruger M, Beger C, Welch PJ, Barber JR, Manns MP, Wong-Staal F. Involvement of proteasome alpha-subunit PSMA7 in hepatitis C virus internal ribosome entry site-mediated translation. Mol Cell Biol 2001;21:8357–64.
217. Ma WJ, Cheng S, Campbell C, Wright A, Furneaux H. Cloning and characterization of HuR, a ubiquitously expressed Elav-like protein. J Biol Chem 1996;271:8144–51.
218. Spangberg K, Wiklund L, Schwartz S. HuR, a protein implicated in oncogene and growth factor mRNA decay, binds to the 3′ ends of hepatitis C virus RNA of both polarities. Virology 2000;274:378–90.
219. Korf M, Jarczak D, Beger C, Manns MP, Kruger M. Inhibition of hepatitis C virus translation and subgenomic replication by siRNAs directed against highly conserved HCV sequence and cellular HCV cofactors. J Hepatol 2005; 43:225–34.
220. Gomez-Gonzalo M, Carretero M, Rullas J, Lara-Pezzi E, Aramburu J, Berkhout B, et al. The hepatitis B virus X protein induces HIV-1 replication and transcription in synergy with T-cell activation signals: functional roles of NF-kappaB/NF-AT and SP1-binding sites in the HIV-1 long terminal repeat promoter. J Biol Chem 2001;276: 35435–43.
221. Gong G, Waris G, Tanveer R, Siddiqui A. Human hepatitis C virus NS5A protein alters intracellular calcium levels, induces oxidative stress, and activates STAT-3 and NF-kappa B. Proc Natl Acad Sci U S A 2001;98:9599–604.
222. Matskevich AA, Strayer DS. Exploiting hepatitis C virus activation of NFkappaB to deliver HCV-responsive expression of interferons alpha and gamma. Gene Ther 2003;10: 1861–73.
223. Strayer DS, Feitelson M, Sun B, Matskevich AA. Paradigms for conditional expression of RNA interference molecules for use against viral targets. Methods Enzymol 2005;392: 227–41.
224. Hamazaki H, Ujino S, Miyano-Kurosaki N, Shimotohno K, Takaku H. Inhibition of hepatitis C virus RNA replication by short hairpin RNA synthesized by T7 RNA polymerase in hepatitis C virus subgenomic replicons. Biochem Biophys Res Commun 2006;343:988–94.
225. Seeger C, Mason WS. Hepatitis B virus biology. Microbiol Mol Biol Rev 2000;64:51–68.
226. Beasley RP, Hwang LY, Lin CC, Chien CS. Hepatocellular carcinoma and hepatitis B virus. A prospective study of 22 707 men in Taiwan. Lancet 1981;2:1129–33.
227. Dienstag JL, Perrillo RP, Schiff ER, Bartholomew M, Vicary C, Rubin M. A preliminary trial of lamivudine for chronic hepatitis B infection. N Engl J Med 1995;333:1657–61.
228. Hadziyannis SJ, Tassopoulos NC, Heathcote EJ, Chang TT, Kitis G, Rizzetto M, et al. Long-term therapy with adefovir dipivoxil for HBeAg-negative chronic hepatitis B. N Engl J Med 2005;352:2673–81.
229. Liaw YF, Sung JJ, Chow WC, Farrell G, Lee CZ, Yuen H, et al. Lamivudine for patients with chronic hepatitis B and advanced liver disease. N Engl J Med 2004;351:1521–31.
230. Marcellin P, Lau GK, Bonino F, Farci P, Hadziyannis S, Jin R, et al. Peginterferon alfa-2a alone, lamivudine alone, and the two in combination in patients with HBeAg-negative chronic hepatitis B. N Engl J Med 2004;351:1206–17.
231. Manesis EK, Hadziyannis SJ. Interferon alpha treatment and retreatment of hepatitis B e antigen-negative chronic hepatitis B. Gastroenterology 2001;121:101–9.
232. McCaffrey AP, Nakai H, Pandey K, Huang Z, Salazar FH, Xu H, et al. Inhibition of hepatitis B virus in mice by RNA interference. Nat Biotechnol 2003;21:639–44.
233. Giladi H, Ketzinel-Gilad M, Rivkin L, Felig Y, Nussbaum O, Galun E. Small interfering RNA inhibits hepatitis B virus replication in mice. Mol Ther 2003;8:769–76.
234. Konishi M, Wu CH, Wu GY. Inhibition of HBV replication by siRNA in a stable HBV-producing cell line. Hepatology 2003;38:842–50.
235. Shlomai A, Shaul Y. Inhibition of hepatitis B virus expression and replication by RNA interference. Hepatology 2003; 37:764–70.
236. Hamasaki K, Nakao K, Matsumoto K, Ichikawa T, Ishikawa H, Eguchi K. Short interfering RNA-directed inhibition of hepatitis B virus replication. FEBS Lett 2003;543:51–4.
237. Ying C, De Clercq E, Neyts J. Selective inhibition of hepatitis B virus replication by RNA interference. Biochem Biophys Res Commun 2003;309:482–4.
238. Klein C, Bock CT, Wedemeyer H, Wustefeld T, Locarnini S, Dienes HP, et al. Inhibition of hepatitis B virus replication in vivo by nucleoside analogues and siRNA. Gastroenterology 2003;125:9–18.
239. Chen Y, Du D, Wu J, Chan CP, Tan Y, Kung HF, et al. Inhibition of hepatitis B virus replication by stably expressed shRNA. Biochem Biophys Res Commun 2003;311:398–404.
240. Wu Y, Huang AL, Tang N, Zhang BQ, Lu NF. Specific antiviral effects of RNA interference on replication and expression of hepatitis B virus in mice. Chin Med J (Engl) 2005; 118:1351–6.
241. Morrissey DV, Blanchard K, Shaw L, Jensen K, Lockridge JA, Dickinson B, et al. Activity of stabilized short interfering RNA in a mouse model of hepatitis B virus replication. Hepatology 2005;41:1349–56.
242. Morrissey DV, Lockridge JA, Shaw L, Blanchard K, Jensen K, Breen W, et al. Potent and persistent in vivo anti-HBV activity of chemically modified siRNAs. Nat Biotechnol 2005;23:1002–7.
243. Uprichard SL, Boyd B, Althage A, Chisari FV. Clearance of hepatitis B virus from the liver of transgenic mice by short hairpin RNAs. Proc Natl Acad Sci U S A 2005;102:773–8.
244. Wu HL, Huang LR, Huang CC, Lai HL, Liu CJ, Huang YT, et al. RNA interference-mediated control of hepatitis B virus and emergence of resistant mutant. Gastroenterology 2005;128:708–16.
245. Carmona S, Ely A, Crowther C, Moolla N, Salazar FH, Marion PL, et al. Effective inhibition of HBV replication in vivo by anti-HBx short hairpin RNAs. Mol Ther 2006;13: 411–21.
246. Kim YH, Lee JH, Paik NW, Rho HM. RNAi-based knockdown of HBx mRNA in HBx-transformed and HBV-producing human liver cells. DNA Cell Biol 2006; 25:412–7.
247. Chen CC, Ko TM, Ma HI, Wu HL, Xiao X, Li J, et al. Long-term inhibition of hepatitis B virus in transgenic mice by double-stranded adeno-associated virus 8-delivered short hairpin RNA. Gene Ther 2007;14:11–9.

Available online at www.sciencedirect.com
ScienceDirect
Journal of Virological Methods 143 (2007) 95–103
Journal of Virological Methods
www.elsevier.com/locate/jviromet

# Optimization of the virus concentration method using polyethyleneimine-conjugated magnetic beads and its application to the detection of human hepatitis A, B and C viruses

Eriko Uchida[a], Mieko Kogi[a,b], Tadashi Oshizawa[a], Birei Furuta[a], Koei Satoh[c], Akiko Iwata[c], Mitsuhiro Murata[d], Mikio Hikata[d], Teruhide Yamaguchi[a,e,*]

[a] *Division of Cellular and Gene Therapy Products, National Institute of Health Sciences, 1-18-1 Kamiyoga, Setagaya, Tokyo 158-8501, Japan*
[b] *Kanazawa Institute of Technology, Nonoichi, Ishikawa, Japan*
[c] *The Institute of the Saitama Red Cross Center, Kumagaya, Saitama, Japan*
[d] *JSR Corporation, Tsukuba Research Laboratories, Tsukuba, Ibaraki, Japan*
[e] *Division of Biological Chemistry and Biologicals, National Institute of Health Sciences, 1-18-1 Kamiyoga, Setagaya, Tokyo 158-8501, Japan*

Received 25 September 2006; received in revised form 22 February 2007; accepted 26 February 2007
Available online 12 April 2007

**Abstract**

To enhance the sensitivity of virus detection by polymerase chain reaction (PCR) and reverse transcription PCR (RT-PCR), a novel virus concentration method using polyethyleneimine (PEI)-conjugated magnetic beads was developed in our previous study. However, several viruses could not be concentrated by this method. In this paper, the conditions of virus concentration were optimized to concentrate a wide range of viruses more efficiently. The PEI beads adsorbed viruses more efficiently than other cationic polymers, and the optimum virus concentration was obtained under weak acidic conditions. Mass spectrometric analysis revealed that several serum proteins, such as complement type 3, complement type 4 and immunoglobulin M (IgM), were co-adsorbed by the PEI beads, suggesting that the beads may adsorb viruses not only by direct adsorption, but also via immune complex formation. This hypothesis was confirmed by the result that poliovirus, which PEI beads could not adsorb directly, could be concentrated by the beads via immune complex formation. On the other hand, hepatitis A (HAV) and hepatitis C (HCV) viruses were adsorbed directly by PEI beads almost completely. Like poliovirus, hepatitis B virus (HBV) was concentrated efficiently by the addition of anti-HBV IgM. In conclusion, virus concentration using PEI beads is a useful method to concentrate a wide range of viruses and can be used to enhance the sensitivity of detection of HAV, HBV and HCV.


*Keywords:* Polyethyleneimine; Virus concentration; Immune complex; HAV; HBV; HCV

## 1. Introduction

Many useful biological/biotechnological medicinal products are produced from biological materials and by cell culture techniques. Recent progress in gene therapy and cell therapy products has provided new hope for the treatment of grave genetic diseases and lethal disorders. These innovative medicinal products, however, involve some risk in terms of the spread of transmissible agents and virus-mediated infectious diseases. To ensure the viral safety of biological/biotechnological products, it is important to confirm that the starting materials, intermediate products and final products are free from virus contamination. This is especially important for cell therapy products, since it is difficult to inactivate and/or remove contaminated viruses from these products.

Polymerase chain reaction (PCR) is a highly sensitive method for the detection of virus genomes (Saiki et al., 1988). Several nucleic acid amplification test (NAT) methods other than PCR have also been developed (Alter et al., 1995; Kamisango et al., 1999; Kern et al., 1996; Notomi et al., 2000; Sarrazin et al., 2000). These tests are reported to be able to detect only some copies of virus genomes. Therefore, in many countries, NAT methods have been employed to detect specific viruses in the virus screening of blood-derived products (Willkommen et al.,

* Corresponding author. Tel.: +81 3 3700 9064; fax: +81 3 3700 9084.
*E-mail address:* yamaguch@nihs.go.jp (T. Yamaguchi).

0166-0934/$ – see front matter © 2007 Elsevier B.V. All rights reserved.
doi:10.1016/j.jviromet.2007.02.014

1999). NAT methods are also thought to be useful in testing biotechnology products derived from cell lines and cell therapy products. However, since all NAT methods used for the detection of viruses have a detection limit, it is impossible to deny virus contamination completely. In order to reduce the virus risk of both biological/biotechnological products and cell therapy products, it is essential to develop more sensitive methods of virus detection. One way to improve the sensitivity of virus detection is to concentrate the target viruses before NAT testing.

Recently, a novel viral concentration method using polyethyleneimine (PEI)-conjugated magnetic beads was developed (Satoh et al., 2003). It was shown that PEI beads efficiently adsorbed many model viruses, such as simian virus 40 (SV-40), herpes simplex 1 virus (HSV-1), Sindbis virus and vesicular stomatitis virus (VSV), and that the method improved the sensitivity of NAT for the detection of virus genomes about 10 to 100 times. It has also been reported that PEI beads efficiently adsorb amphotropic murine leukemia virus, and that the virus concentration method provided sensitive detection of replication-competent retrovirus in retrovirus vector products (Uchida et al., 2004). However, several small non-enveloped viruses such as poliovirus could not be concentrated or were only partially concentrated by PEI beads (Satoh et al., 2003). In addition, the mechanism of virus adsorption by PEI beads remains to be elucidated.

In the present study, the viral concentration method using PEI beads was optimized in order to allow the efficient concentration of several viruses. It was demonstrated that poliovirus can be concentrated by PEI beads via the formation of immune complexes. In addition, it was shown that the virus concentration method using PEI beads is applicable to human infectious viruses such as the hepatitis A(HAV), hepatitis B (HBV) and hepatitis C (HCV) viruses, which are important viruses to test for in order to ensure the viral safety of biological products and cell therapy products.

## 2. Materials and methods

### 2.1. Viruses

SV-40 virus, HSV-1 (stain F), porcine parvovirus (PPV; strain 90HS) and poliovirus (strain Sabin 1) were obtained and amplified as described previously (Satoh et al., 2003). Briefly, the supernatants of Vero cells infected with HSV-1 or poliovirus were used as virus samples. CV-1 cells were infected with SV-40 virus, and 5 days after infection, the supernatant was saved as the SV-40 sample. The supernatant of ESK cells infected with PPV was used as the PPV sample. In order to remove cell debris from the collected virus suspension, each virus suspension was centrifuged at 3000 rpm for 10 min. After removing cell debris, the resulting stock viruses (SV40: $4 \times 10^7$ copies/ml; PPV: $1 \times 10^6$ copies/ml; HSV-1: $1 \times 10^8$ copies/ml; poliovirus: $2 \times 10^7$ copies/ml) were aliquoted and stored at −80 °C until use. Human adenovirus type 5 reference material (ATCC VR-1516; $5.8 \times 10^{11}$ particles/ml) was obtained from the American type culture collection (ATCC) and used without amplification. HAV was obtained from ATCC (strain HM175/18f), infected into FRhK-4 cells, and the supernatant of the cell was saved 9–11 days later as the HAV sample ($1 \times 10^8$ PFU/ml). The first Japanese national standard for HBV DNA (Genotype C; potency: $4.4 \times 10^5$ IU/ml) and the first Japanese national standard for HCV RNA (Mizusawa et al., 2005); genotype HCV-1b; potency: 100,000 IU/ml) were directly used as the HBV sample and HCV sample, respectively.

### 2.2. Preparation of PEI beads

PEI beads were prepared by coupling PEI (MW 70,000; Wako Pure Chemical Industries, Ltd., Tokyo, Japan) with magnetic beads (IMMUTEX-MAG™; mean diameter: 0.8 μm; JSR Inc., Tokyo, Japan) by the 1-ethylene-3-(3-dimethylaminopropyl) carbodiimide coupling method, as described previously (Satoh et al., 2003). The final concentration of the PEI beads was 50 mg/ml. Different molecular weights of PEI beads were prepared as described above but including the coupling of PEI with a molecular weight (MW) of 1800 or PEI (MW 10,000) to magnetic beads, instead of PEI (MW 70,000). Polyarylamine (PAA)-conjugated magnetic beads and poly-L-lysine (PLL)-conjugated magnetic beads were prepared in the same way as PEI beads, using PAA (MW 150,000) or PLL (MW > 300,000) instead of PEI, respectively.

### 2.3. Virus concentration using PEI beads

The essential adsorption procedure for each virus was as follows. Virus samples were diluted with virus dilution medium (Dulbecco's modified Eagle's medium (DMEM) or DMEM supplemented with 2% fetal calf serum (FCS)). The exact concentration of the virus suspension used for each experiment is described in the corresponding figure legends. Next, 1 ml of each virus suspension was incubated with 100 μl of PEI beads for 10 min at room temperature. The complexes of virus and PEI beads were trapped by a magnetic field (Magnetic Trapper™; Toyobo Co., Tokyo, Japan) for 5 min and separated from the supernatant fraction. The virus DNA or RNA was extracted from virus-bead complex or from untreated virus suspensions (100 μl) with an SMI-TEST EX R&D Kit (Medical & Biological Laboratories Co., Nagano, Japan) following the manufacturer's instructions. Extracted DNA or RNA was dissolved in 50 μl of TE buffer (10 mM Tris–HCl (pH 7.4)/0.1 mM EDTA), and 10 μl of the solution was used for real-time PCR or RT-PCR reaction.

### 2.4. Effect of pH on virus concentration by PEI beads

Good's buffers with pH 4–9 (1 M MES, pH 4.0; 1 M MES, pH 5.0; 1 M MES, pH 6.0; 1 M HEPES, pH 7.0; 1 M HEPES, pH 8.0; 1 M Tricine, pH 9.0) were prepared and added to the virus dilution medium at a final concentration of 20 mM. Virus samples were then diluted with the virus dilution media at different pH values, and concentrated with PEI beads as described. The exact concentration of the virus suspension used for each experiment is described in the corresponding figure legends.

### 2.5. Real-time PCR and RT-PCR

Real-time PCR and reverse transcription PCR (RT-PCR) were carried out in a 50-μl reaction mixture containing 10 μl of extracted DNA or RNA, 0.5 μM of each primer set with a fluorescence probe, 25 μl of PCR master mix and, in the case of RT-PCR, a reverse transcriptase mix prepared according to the kit manual. The following real-time PCR and RT-PCR master mix kits were used: a QuantiTect Probe PCR kit (Qiagen, Hilden, Germany) for HSV-1, SV-40, adenovirus and PPV; a QuantiTect Probe RT-PCR kit (Qiagen) for poliovirus, HAV and HCV; and a Platinum Quantitative PCR SuperMix-UDG with ROX (Invitrogen, Carlsbad, CA, USA) for HBV. The 5′-primers, 3′-primers and fluorescence probes used for the real-time PCR and RT-PCR detection of viruses are shown in Table 1. The real-time PCR and RT-PCR were performed on an ABI PRISM 7000 Sequence-Detection System (Applied Biosystems, Foster City, CA, USA).

### 2.6. SDS-PAGE analysis of serum proteins adsorbed on PEI beads

The virus suspension (HSV-1) diluted with DMEM supplemented with 5% FCS was incubated with PEI beads for 10 min. The fraction of serum proteins adsorbed on the beads and the untreated virus suspension were then boiled with sodium dodecyl sulfate (SDS) sample buffer and applied to SDS-polyacrylamide gel electrophoresis (SDS-PAGE). SDS-PAGE was carried out on a slab gel ($T = 7.5\%$) with a BE-120 system from Biocraft (Tokyo, Japan). Protein bands were visualized by Coomassie Brilliant Blue staining.

### 2.7. In-gel digestion

Protein bands of interest were excised from the SDS-PAGE gel, destained three times in 50% acetonitrile and 25 mM ammonium bicarbonate for 10 min each time, and dehydrated in acetonitrile. The gel pieces were dried in a vacuum centrifugal concentrator and incubated with 10 mM dithiothreitol (DTT) in 25 mM ammonium bicarbonate at 56 °C for 60 min. After cooling to room temperature, the DTT solution was replaced with roughly the same volume of 55 mM iodoacetamide in 25 mM ammonium bicarbonate. After incubation for 45 min at room temperature in the dark, the gel pieces were washed in 25 mM ammonium bicarbonate for 5 min and dehydrated by the addition of 50% acetonitrile and 25 mM ammonium bicarbonate for 5 min. After this procedure was repeated twice, the gel pieces were dried in a centrifugal concentrator. The gel pieces were allowed to swell in 2 μl of a digestion buffer containing 25 mM ammonium bicarbonate, 0.1% octyl glucoside, and 25 ng/μl trypsin (sequence grade; Promega, Madison, WI, USA) in ice for 5 min, and then 15 μl of a digestion buffer without trypsin was added. After 30 min, the supernatant was discarded, and the gel pieces were incu-

Table 1
Primer and probe sets used for the real-time PCR and RT-PCR

| Virus | Primer and probe set |
|---|---|
| HSV-1 | Forward primer: 5′-GCGTCATGGTACTGGCAAG-3′<br>Reverse primer: 5′-TTGACTCTACGGAGCTGGCC-3′<br>Probe: 5′-FAM-TGGAGCTGATGCCGTAGTCGG-TAMRA-3′ |
| SV-40 | Forward primer: 5′-GACATTCCTAGGCTCACCTCACA-3′<br>Reverse primer: 5′-ACCTTGCCAAACTGTCCCTTAAA-3′<br>Probe: 5′-FAM-CTTGAAAGAAGAACCCAAAGA-TAMRA-3′ |
| PPV | Forward primer: AACAACTACGCAGCAACTCCAATA-3′<br>Reverse primer: ACGGCTCCAAGGCTAAAGC-3′<br>Probe: 5′-FAM-AGGAGGACCTGGATTT-MGB-3′ |
| Adenovirus*1 | Forward primer: TCCGGTCCTTCTAACACACCTC-3′<br>Reverse primer: ACGGCAACTGGTTTAATGGG-3′<br>Probe: 5′-FAM-TGAGATACACCCGGTGGTCCCGC-TAMRA-3′ |
| Poliovirus | Forward primer: 5′-CCCGAGAAATGGGACGACTA-3′<br>Reverse primer: 5′-TGGAGCTGTTCCGTAGGTGTAA-3′<br>Probe: 5′- FAM-ACATGGCAAACCTCATCAAATCCATCAATC-MGB-3′ |
| HAV*2 | Forward primer: 5′-GGTAGGCTACGGGTGAAAC-3′<br>Reverse primer: 5′-AACAACTCACCAATATCCGC-3′<br>Probe: 5′-FAM-CTTAGGCTAATACTTCTATGAAGAGATGC-TAMRA-3′ |
| HBV*3 | Forward primer: 5′-GGACCCCTGCTCGTGTTACA-3′<br>Reverse primer: 5′-GAGAGAAGTCCACCMCGAGTCTAGA-3′<br>Probe: 5′-FAM-TGTTGACAARAATCCTCACCATACCRCAGA-TAMRA-3′ |
| HCV*4 | Forward primer: 5′-TGCGGAACCGGTGAGTACA-3′<br>Reverse primer: 5′-CTTAAGGTTTAGGATTCGTGCTCAT-3′<br>probe: 5′-FAM-CACCCTATCAGGCAGTACCACAAGGCC-TAMRA-3′ |

Each primer set was prepared according to the original papers described below (*1 to *4) or designed using Primer Express software (Applied Biosystems). *1 Adenovirus (Ishii-Watabe et al., 2003), *2 HAV (Jothikumar et al., 2005), *3 HBV (Pas et al., 2000), *4 HCV (Martell et al., 1999).

bated overnight at 37 °C. To extract tryptic fragments, the gel pieces were shaken in 50% acetonitrile and 5% trifluoroacetic acid (TFA) for 30 min. After this procedure was repeated twice, the extraction solutions were pooled, dried in a centrifugal evaporator, and dissolved in 20 μl of 0.1% TFA. The samples were then absorbed onto reverse-phase ZipTipC18 (Millipore, Bedford, MA, USA). The resin was washed with 0.1% TFA and the peptides were eluted with 3 μl of 75% acetonitrile/0.1% TFA. The eluate was analyzed by mass spectrometry (MS) as described below.

### 2.8. MS and database searching

The peptide mixture (0.5 μl volume) elution was deposited onto a matrix assisted laser desorption/ionization (MALDI) target plate, and this was closely followed by the deposition of 0.5 μl of a saturated solution of α-cyano-4-hydroxycinnamic acid in 50% acetonitrile containing 0.1% TFA. MS and tandem MS (MS/MS) analysis of the peptide mixtures was performed using a 4700 Proteomics Analyzer (Applied Biosystems, Framingham, MA, USA). Peptide mass fingerprinting and MS/MS ion searches were performed for protein identification by a Mascot search based on the MSDB protein database.

### 2.9. Preparation of anti-mouse IgG-rabbit IgM antibody

Anti-mouse immunogloblulin G (IgG) rabbit antiserum was obtained from rabbits immunized with highly purified mouse IgG (11 mg/ml; Jackson ImmunoResearch, West Grove, PA, USA) at 11 days after immunization, when IgM titer was increased. The antiserum (3 ml) was then diluted with an equal volume of phosphate buffered saline (PBS) (−), and applied to a mouse-IgG agarose affinity column (Invitrogen). After washing with 10 ml of PBS (−), the bound fraction was eluted with 0.1 M glycine–HCl (pH 3.0) and neutralized with 1 M Tris–HCl (pH 8.0). A PEI-sepharose-6MB column was prepared by coupling PEI to CNBr-activated sepharose-6MB (GE Healthcare Bioscience, Piscataway, NJ, USA). Anti-mouse IgG rabbit antiserum purified with a mouse IgG-agarose column was applied to a PEI-sepharose-6MB column and washed with PBS (−), and the bound fraction was eluted with 1.4 M NaCl/50 mM HEPES (pH 7.6). The eluted fraction was concentrated and used as anti-mouse IgG rabbit IgM antibody (final concentration, 4 μg/ml).

### 2.10. Poliovirus concentration via immune complexes

When poliovirus suspension was concentrated by PEI beads via immune complex formation, anti-poliovirus 1 mouse monoclonal antibody (IgG1: 5 μl; Chemicon International, Temecula, CA, USA) and purified anti-mouse IgG rabbit IgM antibody (20 μl), or anti-poliovirus 1 mouse monoclonal antibody and human complement C1 (5 μl; Merck Biosciences/Calbiochem, Darmstadt, Germany) and C4 (3 μl; Calbiochem) were added to the virus suspension before incubation with PEI beads.

### 2.11. Preparation of anti-HBV IgM antibody

Anti-hepatitis B surface antigen (HBsAg) IgM antibody was prepared as follows. Rabbits were immunized with a mixture of the adw and adr subtypes of recombinant HBsAg (Advanced ImmunoChemical, Long Beach, CA, USA). Anti-HBsAg rabbit antiserum was obtained at 10 days after immunization, when IgM titer was increased. The antiserum (3 ml) was diluted with an equal volume of PBS (−), applied to a PEI-sepharose-6MB column, washed with 20 ml PBS (−), and eluted with 1.4 M NaCl/100 mM HEPES (pH 7.0). PEI-sepharose-6MB-bound fractions were pooled, desalted with a PD-10 column equilibrated with 1.2 M NaCl/50 mM HEPES buffer (pH 7.4), and purified with an ImmunoPure IgM purification kit (Pierce Biotechnology, Rockford, IL, USA). IgM fractions were concentrated and used as anti-HBsAg IgM antibody.

## 3. Results

### 3.1. Optimization of the virus concentration method using PEI beads

In order to optimize the virus concentration method using PEI beads, the relationship between the MW of PEI coupled with magnetic beads and the efficiency of the virus concentration was examined. When PEIs with average molecular masses of 1800, 10,000 and 70,000 Da were compared, the PEI of MW 70,000 Da efficiently concentrated HSV-1, while magnetic beads with the PEI of MWs 1800 and 10,000 Da could not adsorb HSV-1 (Fig. 1). Therefore, the PEI beads with MW 70,000 Da were used in the following experiments.

Next, the virus adsorption ability of PEI was compared to that of other cationic polymers. As shown in Fig. 2, PEI beads exhibited a markedly higher virus adsorption ability than PAA- or PLL-conjugated magnetic beads for all model viruses tested.

The effect of pH on the efficiency of virus concentration was then examined. HSV-1 and SV-40 virus suspensions at different

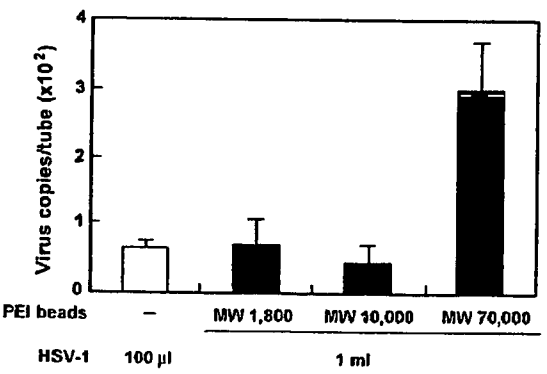


Fig. 1. Comparison of virus concentrations by magnetic beads coupled with PEIs of three different molecular weights. HSV-1 suspension ($1 \times 10^3$ copies/ml, 1 ml/tube) was incubated with PEI beads whose PEI had a molecular weight of 1800, 10,000 or 70,000 Da. Viral genome DNA was extracted from the PEI bead fraction and from untreated HSV-1 suspension (100 μl). Virus copy numbers were determined by real-time PCR. Data are expressed as the mean ± S.D. ($n = 3$).

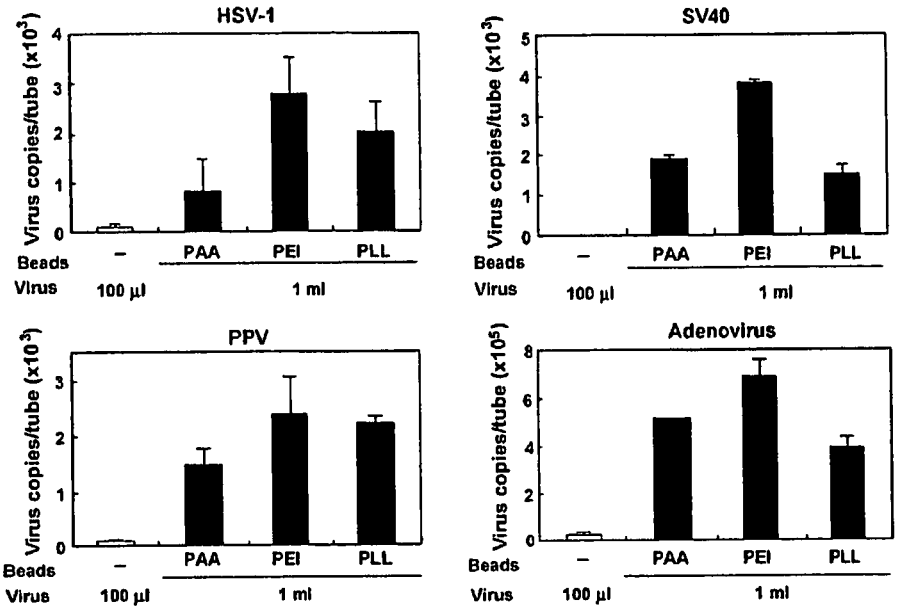


Fig. 2. Comparison of virus concentration by magnetic beads coupled with three different cationic polymers. HSV-1 ($5 \times 10^3$ copies/ml), SV-40 ($5 \times 10^3$ copies/ml), PPV ($5 \times 10^3$ copies/ml) and adenovirus suspensions ($1 \times 10^6$ copies/ml) (1 ml each) were incubated with PAA-, PEI- or PLL-conjugated magnetic beads. Viral genome DNA was extracted from each magnetic bead fraction and from untreated virus suspensions (100 µl each). Virus copy numbers were determined by real-time PCR. Data are expressed as the mean ± S.D. ($n = 3$).

pH levels (pH 5–9) were concentrated by PEI beads following the standard method. A pH levels of 6 was found to be optimal for the concentration of these viruses (Fig. 3).

### 3.2. Analysis of serum proteins adsorbed on PEI beads

To improve the virus concentration method using PEI beads, the serum components co-adsorbed by the beads during virus concentration were analyzed. When a virus suspension containing 5% FCS was concentrated by PEI beads and analyzed by SDS-PAGE, several proteins were specifically adsorbed by the beads (Fig. 4). Using MS and MS/MS analyses of these protein bands, complement type 3, complement type 4 and IgM heavy chain were identified as serum components concentrated by PEI beads. Since complement components and IgM were adsorbed by the beads, it is hypothesized that PEI beads may adsorb viruses not only by direct adsorption, but also via the formation of immune complexes that involve IgM antibody and/or complements.

### 3.3. Concentration of poliovirus by PEI beads via immune complexes

To confirm this hypothesis, concentrations of poliovirus, which PEI beads could not adsorb directly, via the formation of immune complexes were examined. Instead of anti-poliovirus IgM antibody, anti-poliovirus mouse monoclonal antibody (IgG) was used in combination with anti-mouse IgG rabbit IgM anti-

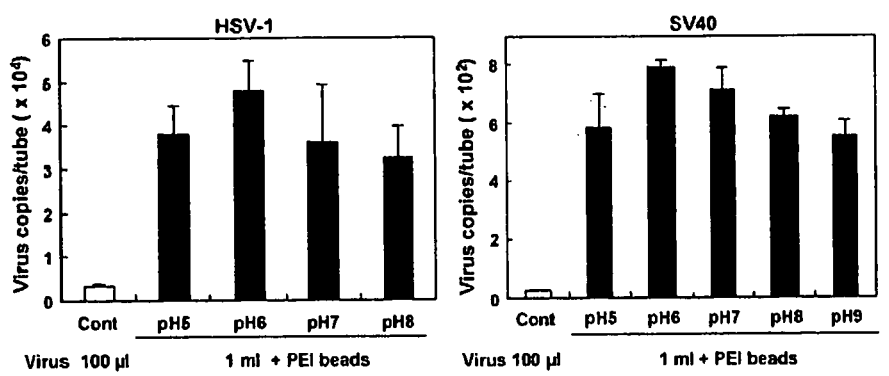


Fig. 3. Effect of pH on the efficiency of virus concentration by PEI beads. HSV-1 ($5 \times 10^4$ copies/ml) and SV-40 ($1 \times 10^3$ copies/ml) suspensions diluted with virus dilution medium at different pH levels (HSV-1: pH 5, 6, 7 and 8; SV-40: pH 5, 6, 7, 8 and 9) (1 ml each) were incubated with PEI beads. Viral genome DNA was then extracted from PEI bead fraction and from untreated virus suspensions (100 µl each). Virus copy numbers were determined by real-time PCR. Data are expressed as the mean ± S.D. ($n = 3$).

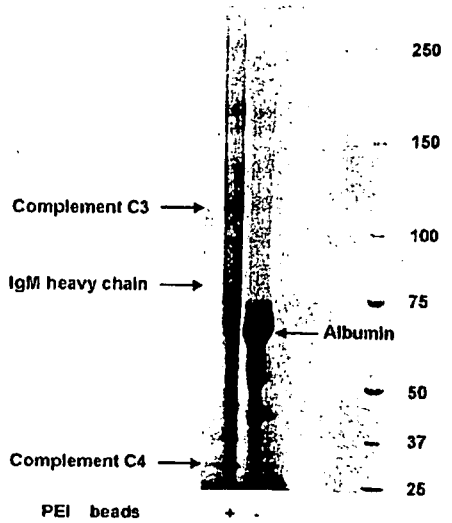


Fig. 4. Serum proteins adsorbed on PEI beads during virus concentration. HSV-1 suspension diluted with DMEM supplemented with 5% FCS was incubated with PEI beads. PEI bead fraction (+) and untreated virus suspension (−) were then boiled with SDS sample buffer and applied to SDS-PAGE. Serum protein bands concentrated by PEI beads were identified by MS/MS analysis, as shown in Fig. 5.

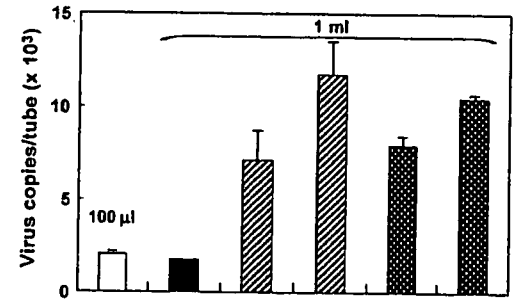


| PEI beads | - | + | + | + | + | + |
|---|---|---|---|---|---|---|
| Anti-poliovirus mouse IgG MoAb | - | - | + | + | + | + |
| Anti-mouse IgG-rabbit IgM | - | - | - | + | - | - |
| C1 + C4 | - | - | - | - | + (r.t.) | + (37°C) |

Fig. 6. Concentration of poliovirus by PEI beads via the formation of immune complexes. Poliovirus suspension ($2 \times 10^4$ copies/ml, 1 ml each) was incubated with PEI beads at room temperature or 37 °C in the absence or presence of anti-poliovirus mouse IgG monoclonal antibody, anti-mouse IgG-rabbit IgM, or a combination of complements C1 and C4. Viral genome RNA was extracted from the PEI bead fraction and from the untreated virus suspension (100 µl). Virus copy numbers were determined by real-time RT-PCR. Data are expressed as the mean ± S.D. ($n = 3$).

body to induce the formation of immune complexes. Anti-mouse IgG rabbit IgM antibody was prepared from rabbit anti-mouse IgG antiserum and purified by a mouse-IgG affinity column followed by a PEI-sepharose-6MB column. Since the PEI-sepharose-6MB column adsorbed IgM (Fig. 5) but not IgG (data not shown), the PEI-sepharose-6MB adsorbed fraction was used as the anti-mouse IgG rabbit IgM antibody. When poliovirus alone was incubated with the PEI beads, it was not adsorbed, but poliovirus was adsorbed when coincubated with anti-poliovirus IgG antibody, and a further significant improvement in the efficiency of virus concentration was achieved by the addition of anti-mouse IgG rabbit IgM along with the anti-poliovirus IgG (Fig. 6). The addition of the combination of complement C1, complement C4 and anti-poliovirus IgG to the reaction mixture of virus and PEI beads also increased the efficiency of virus concentration by PEI beads, but only when the complement system was activated by [incubation at] 37 °C (Fig. 6).

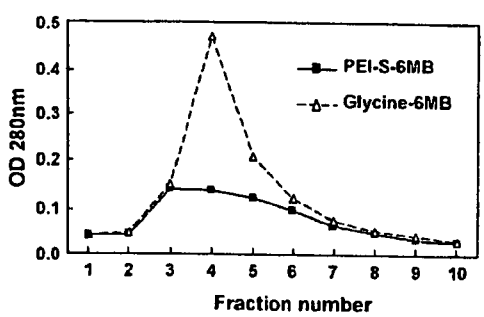


Fig. 5. Adsorption of IgM to a PEI-sepharose column. One ml of human IgM solution (1 mg/ml) was applied to a PEI-sepharose 6MB (PEI-S-6MB) column or to a control column without PEI (Glycine-6 MB) and washed with PBS (−). The eluates were fractionated into ten 1 ml fractions, and the OD280 of each fraction was determined using a spectrophotometer.

### 3.4. Application of the virus concentration method using PEI beads to human hepatitis viruses

The virus concentration method using PEI beads was applied to human HAV, HBV and HCV. Fig. 7 shows the effect of pH on the virus concentration efficiency. HAV was efficiently adsorbed by the PEI beads (Fig. 7A). The number of viral copies obtained in the PEI bead fraction when using 1 ml of virus suspension was about 10-fold the number extracted from untreated virus suspension (100 µl), suggesting that the concentration of HAV almost reached the predicted level. Neither the presence or absence of serum nor the pH condition affected the efficiency of the HAV concentration. HCV was also efficiently adsorbed by PEI beads, even in the presence of 2% FCS, and the optimum pH was found to be 5 (Fig. 7C). On the other hand, the efficiency of HBV concentration by PEI beads was lower than the efficiencies of HAV and HCV concentrations. The number of viral copies obtained in the PEI bead fraction under the optimum condition of pH 5 without serum was about six-fold the number extracted from untreated virus suspension (Fig. 7B). The presence of FCS significantly reduced the adsorption of HBV by PEI beads.

In order to improve the concentration of HBV obtained by PEI beads, anti-HBV IgM antibody was prepared and the concentration of HBV via immune complex formation was examined. As shown in Fig. 8, the concentration of HBV by PEI beads was improved by the addition of anti-HBV IgM antibody. Under the optimum condition, the number of viral copies obtained in the PEI bead fraction was more than seven-fold the number extracted from the untreated virus suspension even in the

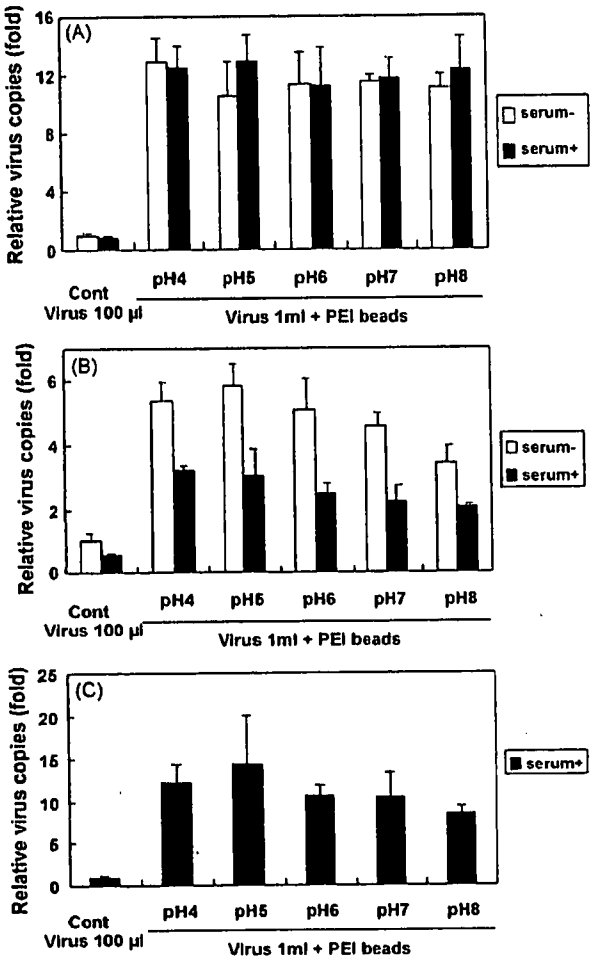


Fig. 7. Effect of pH on the concentration of HAV, HBV and HCV by PEI beads. HAV (A), HBV (B), and HCV (C) were diluted with virus dilution media of different pH levels supplemented with or without 2% FCS. Virus suspensions (HAV: $5 \times 10^4$ PFU/ml; HBV: $8.8 \times 10^3$ IU/ml; HCV: $1 \times 10^3$ IU/ml; 1 ml/tube) with different pH levels were incubated with PEI beads. Viral genome DNA and RNA were then extracted from PEI bead fraction and analyzed by real-time PCR and RT-PCR. Data are expressed as the mean ± S.D. ($n = 3$).

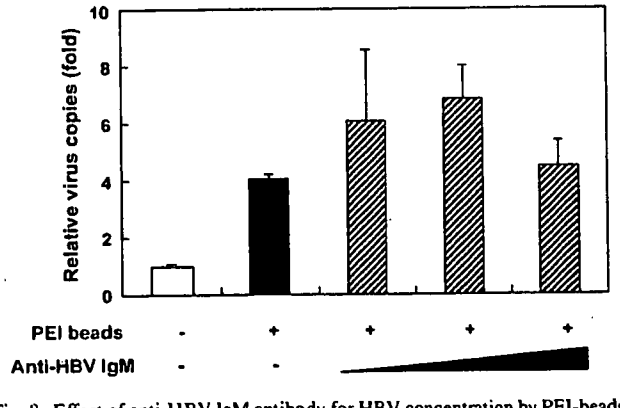


Fig. 8. Effect of anti-HBV IgM antibody for HBV concentration by PEI-beads. HBV suspensions ($8.8 \times 10^3$ IU/ml; 1 ml/tube) were incubated with PEI beads in the absence or presence of 5, 15 or 50 µl of anti-HBV IgM antibody. Viral genome DNA was then extracted from the PEI bead fraction and analyzed by real-time PCR. Data are expressed as the mean ± S.D. ($n = 3$).

presence of serum. Therefore, the virus concentration achieved by PEI beads was shown to be enhanced by the formation of immune complexes.

Table 2 shows a summary of virus concentrations by PEI beads for all of the viruses examined. A wide range of viruses, including small non-enveloped viruses and human hepatitis viruses (HAV, HBV and HCV), were efficiently concentrated by PEI beads under the optimum condition, either directly or by the formation of immune complexes.

## 4. Discussion

In the present study, the virus concentration method using PEI beads (Satoh et al., 2003) was optimized, and was applied to human hepatitis A, B and C viruses.

First, the effects of various cationic polymers, PEI molecular weights, and pH values were examined in order to determine the optimal conditions for virus concentration. Among PEI beads with three different molecular weights (1800, 10,000 and 70,000 Da), only the PEI whose MW was 70,000 Da was able to adsorb viruses (Fig. 1). With respect to the cationic polymers, PEI magnetic beads showed a higher virus adsorption ability than PAA- or PLL-conjugated magnetic beads (Fig. 2). The optimum pH for the concentration of model viruses by PEI beads was subacidic (Fig. 3). The virus adsorption mechanism of PEI beads remains unclear. However, it is hypothesized that the positively charged field of the PEI molecule may interact tightly with the negative charge of surface lipids or the negatively charged surface proteins on viruses (Satoh et al., 2003). PEI is a polycationic polyamine with the highest cationic charge density among existing polymers (Futami et al., 2005). PEI has a branched backbone containing primary, secondary and tertiary amine groups. In contrast, PAA is a linear polycation having only primary amine groups, and PLL is a linear polycation with primary and secondary amine groups. Therefore, it is suggested that the high-density cationic charge of PEI and its branched structure on the surface of the magnetic beads may be important for efficient virus adsorption. According to the analysis of Owada et al. (1999), the interaction between PEI-coated membranes and human immunodeficiency virus type 1 (HIV-1) or plasma protein may be dependent on the surface area of each particle, and this fundamental principle was consistent with their observation that PEIs with higher MWs bound more intensely to HIV-1. This is also consistent with the data that PEI with a MW of 70,000 Da was able to adsorb viruses more efficiently than PEIs of 1800 Da or 10,000 Da.

In order to improve the efficiency of virus concentration by PEI beads, the serum components co-adsorbed by the beads were analyzed. MS analysis revealed that several proteins, including complement type 3, complement type 4 and IgM, were specifically co-adsorbed by PEI beads during virus concentration (Fig. 4), suggesting that the beads were able to adsorb immune complexes that involved IgM antibody and/or complements. Therefore, it is hypothesized that in addition to direct adsorption, PEI beads may adsorb viruses via the formation of immune complexes. This hypothesis was confirmed by the fact that PEI beads were able to adsorb poliovirus under con-

Table 2
Summary of concentration of viruses by PEI beads

| Viruses | Natural host | Virus genome | Envelope | Size (nm) | PEI beads concentration |
|---|---|---|---|---|---|
| Model viruses cytomegalovirus (CMV) | Simian | DNA | + | 180–200 | + |
| Herpes symplex virus type 1 (HSV-1) | Human | DNA | + | 150–200 | + |
| Vesicular stomatitis virus (VSV) | Bovine | RNA | + | 70–150 | + |
| Amphotropic murine leukemia virus | Murine | RNA | + | 80–110 | + |
| Sindbis virus | Human | RNA | + | 60–70 | + |
| Adenovirus type 5 | Human | DNA | – | 70–90 | + |
| Simian virus 40 (SV40) | Simian | DNA | – | 40–50 | + |
| Porcine parvovirus (PPV) | Porcine | DNA | – | 18–24 | + |
| Poliovirus sabin 1 | Human | RNA | – | 25–30 | +[a] |
| Human hepatitis viruses hepatitis B virus (HBV) | Human | DNA | + | 40–45 | +[a] |
| Hepatitis C virus (HCV) | Human | RNA | + | 40–50 | + |
| Hepatitis A virus (HAV) | Human | RNA | – | 25–30 | + |

[a] Concentrated by the addition of antibodies.

ditions which fostered immune complex formation, such as the addition of anti-poliovirus mouse IgG antibody with anti-mouse IgG rabbit IgM, or the addition of anti-poliovirus IgG antibody with activated complements (Fig. 6). Poliovirus is a very small (25–30 nm) non-enveloped virus, and could not be concentrated by PEI beads in our previous study (Satoh et al., 2003). Another possible explanation is that the increase in the surface area of virus particles due to the formation of immune complexes enhances the interaction between the poliovirus and the PEI beads, as hypothesized by Owada et al. (1999).

The results obtained from model viruses suggest that the virus concentration method using PEI beads may be applicable to a wide range of viruses. Therefore, this method was applied to human hepatitis viruses. A recent study reported that in some HAV patients, the duration of the viremic phase persisted for more than 1 year with low viral load levels ($10^3$–$10^4$ HAV genome equivalents/ml) (Normann et al., 2004). In the case of HBV, the presence of occult HBV infection (HBV DNA positivity in the setting of negative serum hepatitis B surface antigen) has been documented, and the majority of these infections were associated with low viral loads (<$10^5$ copies/ml) (Minuk et al., 2004). Several studies have demonstrated high rates of transmission of HCV through transfusions with extremely low viral loads (Operskalski et al., 2003). HCV is particularly infectious during the early window period, with levels as low as 1 viral copy in 20 ml plasma able to transmit infection by transfusion (Busch et al., 2003), though intermittent low-level HCV viremia can occur as long as 2 months before the periods of exponential increase in viral load (Glynn et al., 2005). Therefore, it is extremely important to develop a highly sensitive detection method for these viruses. In the present study, it was possible to concentrate HAV and HCV by PEI-beads to almost the predicted levels (Fig. 7). In contrast, HBV was not fully concentrated even under optimum conditions around pH 5. Therefore, the concentration of HBV via the formation of immune complexes was tested. As expected, the concentration of HBV was improved by the addition of anti-HBV IgM antibody (Fig. 8), indicating that the virus concentration method using PEI beads is applicable for the concentration and sensitive detection of HAV, HBV and HCV by PCR and RT-PCR reaction.

To enhance/establish the utility of this virus concentration method using PEI meads for viral safety of biological products and cell therapy products, examination using actual patient sera and different genotypes/subtypes of each virus may be required. In a preliminary experiment, it is confirmed that this PEI beads method can be used for hepatitis virus samples spiked in human plasma. Applicability to different genotypes will be examined using a Japanese genotype panel of HBV and HCV, which will be available soon.

PEI beads may be applicable not only for virus concentration but also for the efficient infection of viruses. Scherer et al. (2002) report that superparamagnetic nanoparticles coated with PEI enhanced the infection of adenovirus and retrovirus vectors under a magnetic field. This infection method (magnetofection) also enhanced the infection of measles virus (Kadota et al., 2005). In a preliminary experiment, the PEI beads used in the present study also enhanced the infectivity of several viruses under a magnetic field. Therefore, it is suggested that PEI beads may be useful for the sensitive detection of both virus genomes and virus infectivity.

In conclusion, the present study demonstrates that the virus concentration method using PEI beads is effective for the concentration and sensitive detection of a wide range of viruses, including HAV, HBV and HCV.

## Acknowledgements

This work was supported in part by a Grant-in-Aid for Health and Labor Science Research (H17-SAISEI-021) from the Japanese Ministry of Health, Labor and Welfare, as well as by a Grant-in-Aid for Research on Health Sciences focusing on Drug Innovation from the Japan Health Sciences Foundation. The authors are grateful to Ms. Momoko Komesu for her technical assistance.

## References

Alter, H.J., Sanchez-Pescador, R., Urdea, M.S., Wilber, J.C., Lagier, R.J., Di Bisceglie, A.M., Shih, J.W., Neuwald, P.D., 1995. Evaluation of branched DNA signal amplification for the detection of hepatitis C virus RNA. J. Viral Hepat. 2, 121–132.

Busch, M.P., Hirschkorn, D.F., Herring, B.L., Delwart, E.L., McAuley, J., Murthy, K.K., Alter, H.J., 2003. Defining the minimal infectious dose and infectious wind[o]w period for HCV using plasma donor panels and the chimpanzee transfusion model. Transfusion 43, S107–S140.

Futami, J., Kitazoe, M., Maeda, T., Nukui, E., Sakaguchi, M., Kosaka, J., Miyazaki, M., Kosaka, M., Tada, H., Seno, M., Sasaki, J., Huh, N.H., Namba, M., Yamada, H., 2005. Intracellular delivery of proteins into mammalian living cells by polyethylen[e]imine-cationization. J. Biosci. Bioeng. 99, 95–103.

Glynn, S.A., Wright, D.J., Kleinman, S.H., Hirschkorn, D., Tu, Y., Heldebrant, C., Smith, R., Giachetti, C., Gallarda, J., Busch, M.P., 2005. Dynamics of viremia in early hepatitis C virus infection. Transfusion 45, 994–1002.

Ishii-Watabe, A., Uchida, E., Iwata, A., Nagata, R., Satoh, K., Fan, K., Murata, M., Mizuguchi, H., Kawasaki, N., Kawanishi, T., Yamaguchi, T., Hayakawa, T., 2003. Detection of replication-competent adenoviruses spiked into recombinant adenovirus vector products by infectivity PCR. Mol. Ther. 8, 1009–1016.

Jothikumar, N., Cromeans, T.L., Sobsey, M.D., Robertson, B.H., 2005. Development and evaluation of a broadly reactive TaqMan assay for rapid detection of hepatitis A virus. Appl. Environ. Microbiol. 71, 3359–3363.

Kadota, S., Kanayama, T., Miyajima, N., Takeuchi, K., Nagata, K., 2005. Enhancing of measles virus infection by magnetofection. J. Virol. Meth. 128, 61–66.

Kamisango, K., Kamogawa, C., Sumi, M., Goto, S., Hirao, A., Gonzales, F., Yasuda, K., Iino, S., 1999. Quantitative detection of hepatitis B virus by transcription-mediated amplification and hybridization protection assay. J. Clin. Microbiol. 37, 310–314.

Kern, D., Collins, M., Fultz, T., Detmer, J., Hamren, S., Peterkin, J.J., Sheridan, P., Urdea, M., White, R., Yeghiazarian, T., Todd, J., 1996. An enhanced-sensitivity branched-DNA assay for quantification of human immunodeficiency virus type 1 RNA in plasma. J. Clin. Microbiol. 34, 3196–3202.

Martell, M., Gomez, J., Esteban, J.I., Sauleda, S., Quer, J., Cabot, B., Esteban, R., Guardia, J., 1999. High-throughput real-time reverse transcription-PCR quantitation of hepatitis C virus RNA. J. Clin. Microbiol. 37, 327–332.

Minuk, G.Y., Sun, D.F., Greenberg, R., Zhang, M., Hawkins, K., Uhanova, J., Gutkin, A., Bernstein, K., Giulivi, A., Osiowy, C., 2004. Occult hepatitis B virus infection in a North American adult hemodialysis patient population. Hepatology 40, 1072–1077.

Mizusawa, S., Okada, Y., Horiuchi, Y., Tanaka, T., Sato, K., Kaneko, K., Sasaki, Y., Tanaka, T., Tomono, T., Tomomizu, T., Hayami, S., Hijikata, M., Hirako, I., Mayumi, M., Mikami, K., Mishiro, S., Miyamoto, S., Muta, K., Weimer, T., Gierman, T., Komuro, K., Yamaguchi, T., 2005. Establishment of the first national standard for nucleic acid amplification technology assay for HCV RNA. Jpn. J. Transfus. Med. 51, 515–519.

Normann, A., Jung, C., Vallbracht, A., Flehmig, B., 2004. Time course of hepatitis A viremia and viral load in the blood of human hepatitis A patients. J. Med. Virol. 72, 10–16.

Notomi, T., Okayama, H., Masubuchi, H., Yonekawa, T., Watanabe, K., Amino, N., Hase, T., 2000. Loop-mediated isothermal amplification of DNA. Nucl. Acids Res. 28, E63.

Operskalski, E.A., Mosley, J.W., Tobler, L.H., Fiebig, E.W., Nowicki, M.J., Mimms, L.T., Gallarda, J., Phelps, B.H., Busch, M.P., 2003. HCV viral load in anti-HCV-reactive donors and infectivity for their recipients. Transfusion 43, 1433–1441.

Owada, T., Miyashita, Y., Motomura, T., Onishi, M., Yamashita, S., Yamamoto, N., 1999. Anti-HIV-1 activity of an ionically modified porous polypropylene membrane determined by filtration of a viral suspension. Microbiol. Immunol. 43, 141–151.

Pas, S.D., Fries, E., De Man, R.A., Osterhaus, A.D., Niesters, H.G., 2000. Development of a quantitative real-time detection assay for hepatitis B virus DNA and comparison with two commercial assays. J. Clin. Microbiol. 38, 2897–2901.

Saiki, R.K., Gelfand, D.H., Stoffel, S., Scharf, S.J., Higuchi, R., Horn, G.T., Mullis, K.B., Erlich, H.A., 1988. Primer-directed enzymatic amplification of DNA with a thermostable DNA polymerase. Science 239, 487–491.

Sarrazin, C., Teuber, G., Kokka, R., Rabenau, H., Zeuzem, S., 2000. Detection of residual hepatitis C virus RNA by transcription-mediated amplification in patients with complete virologic response according to polymerase chain reaction-based assays. Hepatology 32, 818–823.

Satoh, K., Iwata, A., Murata, M., Hikata, M., Hayakawa, T., Yamaguchi, T., 2003. Virus concentration using polyethyleneimine-conjugated magnetic beads for improving the sensitivity of nucleic acid amplification tests. J. Virol. Meth. 114, 11–19.

Scherer, F., Anton, M., Schillinger, U., Henke, J., Bergemann, C., Kruger, A., Gansbacher, B., Plank, C., 2002. Magnetofection: enhancing and targeting gene delivery by magnetic force in vitro and in vivo. Gene Ther. 9, 102–109.

Uchida, E., Sato, K., Iwata, A., Ishii-Watabe, A., Mizuguchi, H., Hikata, M., Murata, M., Yamaguchi, T., Hayakawa, T., 2004. An improved method for detection of replication-competent retrovirus in retrovirus vector products. Biologicals 32, 139–146.

Willkommen, H., Schmidt, I., Lower, J., 1999. Safety issues for plasma derivatives and benefit from NAT testing. Biologicals 27, 325–331.

Leukemia (2007), 1–10

www.nature.com/leu

ORIGINAL ARTICLE

# Proteome analyses of the growth inhibitory effects of NCH-51, a novel histone deacetylase inhibitor, on lymphoid malignant cells

T Sanda[1,2], T Okamoto[1], Y Uchida[1], H Nakagawa[3], S Iida[2], S Kayukawa[2], T Suzuki[3], T Oshizawa[4], T Suzuki[4], N Miyata[3] and R Ueda[2]

*[1]Department of Molecular and Cellular Biology, Nagoya City University Graduate School of Medical Sciences, Nagoya, Japan; [2]Department of Internal Medicine and Molecular Science, Nagoya City University Graduate School of Medical Sciences, Nagoya, Japan; [3]Department of Organic and Medicinal Chemistry, Nagoya City University Graduate School of Pharmaceutical Sciences, Nagoya, Japan and [4]Department of Cellular and Gene Therapy Products, National Institute of Health Sciences, Tokyo, Japan*

**Recent reports showing successful inhibition of cancer and leukemia cell growth using histone deacetylase inhibitor (HDACi) compounds have highlighted the potential use of HDACi as anti-cancer agents. However, high incidence of toxicity and low stability *in vivo* were observed with hydroxamic acid-based HDACi such as suberoylanilide hydroxamic acid (SAHA), thus limiting its clinical applicability. In this study, we found that a novel non-hydroxamate HDACi NCH-51 could inhibit the cell growth of a variety of lymphoid malignant cells through apoptosis induction, more effectively than SAHA. Activation of caspase-3, -8 and -9, but not -7 was detected after the treatment with NCH-51. Gene expression profiles showed that NCH-51 and SAHA similarly upregulated *p21* and downregulated anti-apoptotic molecules including *survivin*, *bcl-w* and *c-FLIP*. Proteome analysis using two-dimensional electrophoresis revealed that NCH-51 upregulated anti-oxidant molecules including peroxiredoxin 1 and 2 and glutathione *S*-transferase at the protein level. Interestingly, NCH-51 induced reactive oxygen species (ROS) after 8 h whereas SAHA continuously declined ROS. Pretreatment with an antioxidant, *N*-acetyl-L-cysteine, abolished the cytotoxicity of NCH-51. These findings suggest that NCH-51 exhibits cytotoxicity by sustaining ROS at the higher level greater than SAHA. This study indicates the therapeutic efficacy of NCH-51 and novel insights for anti-HDAC therapy.**
*Leukemia* advance online publication, 9 August 2007; doi:10.1038/sj.leu.2404902
**Keywords:** histone deacetylase; apoptosis; reactive oxygen species; peroxiredoxin

## Introduction

Histone deacetylase (HDAC) is responsible for deacetylation of histone or non-histone substrates.[1–3] Deacetylation of histone converts local chromatin into repressive configuration, resulting in the transcriptional repression.[2,3] The aberrant recruitment of HDAC is closely associated with leukemogenesis through silencing of expression of the genes involved in hematopoietic cell differentiation.[4] In addition, subsequent studies demonstrated that the malignant phenotypes of solid tumors could be ascribed to the aberrant activation of HDAC and deacetylation of the histone proteins adjacent to tumor suppressor genes.[5,6] Thus, a number of small-molecule HDAC inhibitors (HDACi) have been developed as anti-cancer agents.[1,7] In fact, HDACi compounds were shown to induce cell cycle arrest, differentiation and apoptosis in a variety of malignant cells.[1,7]

Suberoylanilide hydroxamic acid (SAHA) (also known as vorinostat) belongs to a hydroxamic acid-based hybrid polar compound and is a prototypic compound of HDACi.[7] Phase I clinical trials with refractory solid tumors and hematological malignancies by SAHA revealed frequent toxicities including dehydration, fatigue, diarrhea, anorexia and cytopenia, in spite of significant clinical benefits.[8] In addition, a poor pharmacokinetics of SAHA was noted.[8] Other hydroxamic acid-based derivatives showed similar therapeutic profiles.[9,10] Thus, we have attempted to develop a non-hydroxamate HDACi to overcome these problems. A novel HDACi NCH-51 was designed based on SAHA by replacement of the hydroxamic acid by acylated thiol group. NCH-51 could inhibit HDACs as strongly as SAHA and inhibited the cell growth of various solid tumor cell lines *in vitro* (mean $IC_{50}$ values of NCH-51 and SAHA are 3.8 and 3.7 $\mu$M, respectively).[11] Unlike SAHA, NCH-51 is stable in human plasma at the remaining rate of approximately 51% after 24 h of administration (unpublished data).

Recent findings suggest that HDACi may have additional effects other than transcriptional interference. Although it is well established that HDACi upregulates gene expression of tumor suppressors such as *p21* through histone hyperacetylation,[12–14] HDACi does not always upregulate gene expression but induces malignant cell death by downregulating gene expression such as anti-apoptotic genes. In addition, some HDACi compounds exhibited anti-cancer effects through acetylation of non-histone substrates such as heat-shock protein 90 (HSP90),[15] α-tubulin,[16] p53[17] and nuclear factor-κB.[18] For example, Bali *et al.*[15] reported that HDACi caused leukemia cell death by hyperacetylation of HSP90. Hideshima *et al.*[19] demonstrated that tubacin, a specific HDAC6 inhibitor, was effective in augmenting cell death mediated by bortezomib, a proteasome inhibitor, by inhibiting the protein degradation through blocking aggresome activity. Thus, the cell growth inhibitory action of HDACi could be exhibited at the protein expression level.

Here we demonstrate the therapeutic efficacy of NCH-51 on lymphoid malignant cells. NCH-51 induced cell death, more strongly than SAHA. We analyzed the protein expression profiles and found that NCH-51 modulated the expression of antioxidant molecules at the protein level. NCH-51 sustained the intracellular reactive oxygen species (ROS) greater than SAHA.

Correspondence: Professor T Okamoto, Department of Molecular and Cellular Biology, Nagoya City University Graduate School of Medical Sciences, 1 Kawasumi, Mizuho-cho, Mizuho-ku, Nagoya, Aichi 467-8601, Japan.
E-mail: tokamoto@med.nagoya-cu.ac.jp
Received 22 March 2007; revised 6 June 2007; accepted 11 July 2007

a

| Cell type | | Cell line name | 24h | | 72h | |
|---|---|---|---|---|---|---|
| | | | SAHA | NCH-51 | SAHA | NCH-51 |
| T-cell | T-ALL | Jurkat | 0.90 | 0.72 | 0.63 | 0.75 |
| | ATL | MT-2 | >30.00 | 7.81 | 0.54 | 2.08 |
| | | ATL-102 | >30.00 | 5.80 | 1.70 | 2.25 |
| | | ED-40515 (-) | 1.43 | 0.84 | 0.90 | 0.76 |
| B-cell | CLL | MEC2 | >30.00 | 0.71 | 0.70 | 0.87 |
| | | MO1043 | >30.00 | 7.67 | 0.76 | 0.79 |
| | BL | Raji | >30.00 | 1.65 | 0.84 | 0.71 |
| | | Daudi | >30.00 | >30.00 | >30.00 | 1.42 |
| | MM | U266 | 7.67 | 1.36 | 0.53 | 0.66 |
| | | XG7 | >30.00 | 2.00 | 0.73 | 1.11 |
| | | KMS | >30.00 | >30.00 | 1.35 | 3.48 |
| | | ILKM-2 | 1.41 | 1.11 | 0.61 | 0.66 |
| | | RPMI8226 | 5.72 | 1.00 | 2.92 | 2.72 |

Growth inhibition (%)
80-100
60-80
40-60
20-40
0-20

Each Value means $IC_{50}$

b

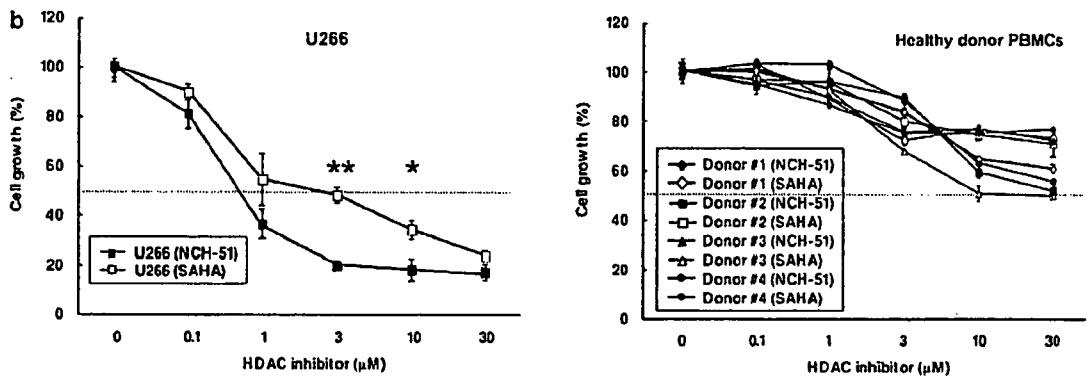


c

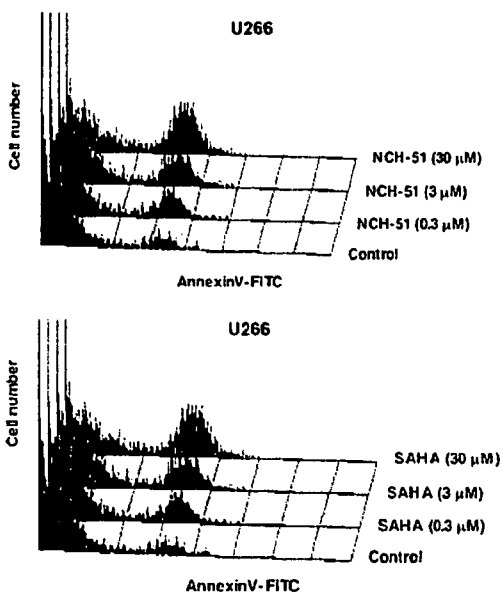


d

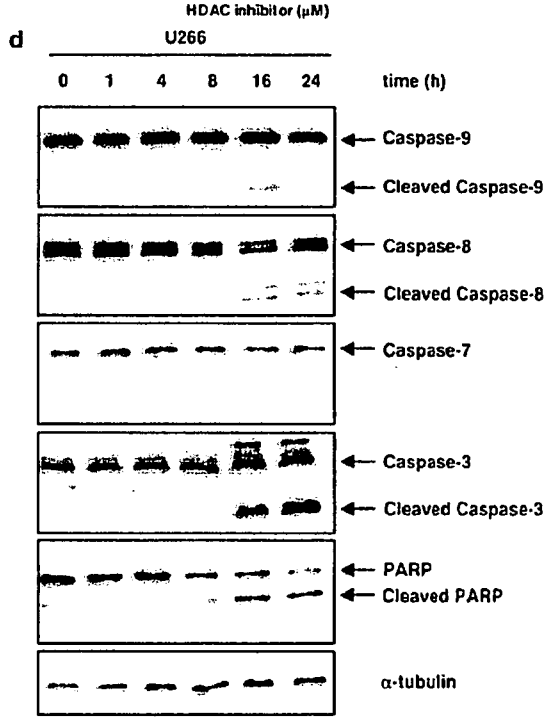

## Materials and methods

### *Cell lines and reagents*

A human acute T-cell leukemia cell line, Jurkat, ATL cell lines, MT-2, ATL-102 and ED-40515(−), chronic lymphocytic leukemia cell lines, MEC2 and MO1043, Burkitt's lymphoma cell lines, Raji and Daudi and multiple myeloma cell lines, U266, XG7, KM5, ILKM-2 and RPMI-8226 were used in this study as described previously.[20–24] For normal controls, peripheral blood mononuclear cells (PBMCs) were obtained from four independent healthy donors upon informed consent after the approval of Institutional Ethical Committee. All cells were cultured in RPMI-1640 medium, supplemented with 10% fetal bovine serum at 37°C in a 5% $CO_2$ incubator. NCH-51, a novel non-hydroxamate HDACi, and SAHA, a conventional hydroxamate HDACi, were synthesized by us as described previously.[11] NCH-51 and SAHA were dissolved in dimethyl sulfoxide at 50 mM and stored at −20°C. An antioxidant compound *N*-acetyl-L-cysteine (NAC) was purchased from Sigma (St Louis, MS, USA).

### *Growth inhibition assay*

Growth inhibitory effect of HDACi was determined using 3-(4,5-dimethylthiazol-2-yl)-2,5-diphenyltetrazolium bromide assay (Sigma) as described previously.[25] Briefly, approximately $1–10 \times 10^4$ cells per 100 $\mu$l were cultured in 96-well plate in triplicates at 37°C. Optical densities (OD) at 570 and 630 nm were measured with a multiplate reader. Cell growth (%) was calculated as follows: ($OD_{630}$–$OD_{570}$ of the samples/$OD_{630}$–$OD_{570}$ of the control) × 100.

### *Apoptosis and cell cycle analysis*

Apoptosis and cell cycle analyses were performed as described previously.[20] For apoptosis analysis, the cells were treated with or without HDACi for 18 h, and incubated with fluorescein isothiocyanate (FITC)-conjugated annexin V (MBL, Nagoya, Japan). The cell numbers of annexin V-positive cells were analyzed by flowcytometry (FACScan, BD Bioscience, San Jose, CA, USA) and CellQuest analysis program (BD Bioscience). For cell cycle analysis, the cells were incubated with or without HDACi for 24 h, washed with cold phosphate-buffered saline (PBS), and fixed with 70% ethanol. After incubation with RNase A (Qiagen, Alameda, CA, USA), the cell pellets were resuspended in PBS containing propidium iodide (Sigma). DNA content of each cell preparation was analyzed by flowcytometry.

### *Protein extraction for proteome analysis*

Proteome analysis was performed according to Seike *et al.*[26] U266 cells were incubated with or without 3 $\mu$M NCH-51 for 18 h. The cell pellets were washed with cold PBS and then treated with 10%trichloroacetic acid for 30 min on ice. After washing with PBS, the pellets were collected and resuspended in lysis buffer (30 mM Tris–HCl (pH, 8.5), 7 M urea, 2 M thiourea, 3% 3-((3-chlamidopropyl) dimethylammonio)-1-propanesulfonic acid and 1% Triton X-100). Samples were then subjected to a Dounce homogenizer for 30 strokes and sonicated for 5 min in a sonicator (UCW-201, Cosmobio Co. Ltd., Tokyo, Japan). After incubation for 30 min, the samples were centrifuged at $10\,000 \times g$ for 30 min followed by ultracentrifugation at $100\,000 \times g$ for 1 h, and the supernatants were collected. Protein concentration was determined by 2D-Quant kit (GE Healthcare Bio-Sciences Corp., Piscataway, NJ, USA). Fifty micrograms of each protein extract, adjusted to pH 8.5, were labeled with 200 pmol of minimal dye CyDye (GE Healthcare Bio-Sciences Corp.). NCH-51-treated samples and untreated control proteins were labeled with Cy3 and Cy5, respectively. Internal control, consisting of half part of each paired sample was labeled with Cy2. Labeling reaction was stopped with the addition of 0.2 mM L-lysine (Sigma) for 10 min on ice. Each labeled sample was mixed into one tube and then incubated with an equal amount of lysis buffer for 10 min on ice. The final volume was adjusted to 450 $\mu$l with DeStreak Rehydration Solution and 0.5% IPG buffer (GE Healthcare Bio-Sciences Corp.).

### *Two-dimensional (2D) electrophoresis and image analysis*

An immobilized pH gradient gel Immobiline DryStrip (GE Healthcare Bio-Sciences Corp.), with non-linear pH values (3–10), was rehydrated with the labeled protein samples at 20°C for 12 h. Isoelectric focusing was performed using IPGphor (GE Healthcare Bio-Sciences Corp.) at 20°C for total 65 000 khT. Immobiline DryStrips were then equilibrated for 15 min in the buffer (6 M urea, 1.5 M Tris–HCl (pH 8.8), 30% glycerol, 2% sodium dodecyl sulfate) containing 10 mg/ml dithiothreitol and prolonged for 15 min in the same buffer containing 25 mg/ml iodoacetamide. After equilibration, Immobiline DryStrips were transferred onto 11.5% polyacrylamide gels and run in the EttanDalt Six system (GE Healthcare Bio-Sciences Corp.) at 30 W/gel for 5 h at 20°C. The gels were scanned with appropriate wavelengths for excitation and emission using Ettan DIGE Primo (GE Healthcare Bio-Sciences Corp.). Relative quantification of spot intensities and statistical evaluation were carried out with ImageMaster 2D Platinum software (GE Healthcare Bio-Sciences Corp.). The experiments were performed in quadruplicates. The protein spots that were statisti-

**Figure 1** Induction of apoptosis by a novel HDAC inhibitor NCH-51. (a) The growth inhibitory effects of NCH-51 and suberoylanilide hydroxamic acid (SAHA) on 13 lymphoid malignant cell lines. The cells were treated with either NCH-51 or SAHA (3 $\mu$M) for 24 or 72 h. Cell growth was estimated by 3-(4,5-dimethylthiazol-2-yl)-2,5-diphenyltetrazolium bromide (MTT) assay and gray-scale levels represent the growth inhibition rate (%) compared to untreated control. Each value indicates the mean $IC_{50}$. (b) Growth inhibitory effects of NCH-51 and SAHA on U266 cells and four control peripheral blood mononuclear cells (PBMCs). A multiple myeloma cell line U266 cells, and four healthy donor PBMCs were treated with indicated concentrations (0–30 $\mu$M) of NCH-51 (closed symbols) or SAHA (opened symbols) for 24 h. Cell growth was evaluated by MTT assay. The results are shown as the percentage cell growth compared to untreated control. These experiments were performed in triplicates and the mean values ± s.d. are shown. $^*P<0.05$; $^{**}P<0.01$. (c) Induction of apoptosis by NCH-51. U266 cells were treated with the indicated concentrations (0–30 $\mu$M) of NCH-51 for 18 h, stained with fluorescein isothiocyanate-conjugated annexin V, and analyzed by flowcytometry. Annexin V-positive fraction indicates the cells undergoing apoptosis. (d) Activation of caspases and poly-ADP ribose polymerase (PARP) cleavage by NCH-51. U266 cells were treated with 3 $\mu$M of NCH-51 for 0–24 h. Whole cell extracts were prepared and subjected to immunoblots with the indicated antibodies. Positions of uncleaved (inactivated) and cleaved (activated) caspases and PARP proteins are indicated by arrows.

cally significant between untreated control and treated sample were selected.

### Protein identification by mass spectrometry

For mass spectrometric analysis, 400 μg of unlabeled-protein extract was independently applied to 2D electrophoresis. The gel was stained with DeepPurple solution (GE Healthcare Bio-Sciences Corp.) according to the manufacturer's recommendation. The gel image was obtained by scanning with Ettan DIGE Primo and matched to those of analytical gels by using the ImageMaster 2D Platinum software. The spots of interest were picked out, and in-gel protein digestion was carried out with trypsin gold (Promega, Madison, WI, USA) as described.[26] Mass spectrometric analyses were performed by using a MALDI-TOF/TOF type mass spectrometer AB4700 (Applied Biosystems, Framingham, MA, USA). The proteins were identified through the online search using MASCOT database search engine.

### Immunoblot analysis

The cell extracts obtained from cell cultures treated with or without HDACi were subjected to cell extract preparation as described above. The samples were applied to electrophoresis on a 10% polyacrylamide gel and transferred onto a nitrocellulose membrane. The membranes were incubated in TBS-T (10 mM Tris–HCl (pH, 8.0), 150 mM NaCl, 0.1% Tween) with 5% non-fat milk containing 1:1000 diluted primary antibodies against either caspase-9, -8, -7, -3, poly-ADP ribose polymerase (PARP) (Cell Signaling Technology, Danvers, MA, USA), peroxiredoxin 1 (Affinity Bioreagents, Golden, CO, USA), elongation factor-2 or α-tubulin (Santa Cruz, Santa Cruz, CA, USA). Membranes were then rinsed in TBS-T and further incubated with HRP-conjugated secondary antibody (GE Healthcare Bio-Sciences Corp.) in TBS-T with 5% non-fat milk. Each protein was detected by SuperSignal (PIERCE, Rockford, IL, USA).

### Detection of ROS

ROS content was measured as described previously.[27] After treatment with HDACi, the cells were incubated with an oxidation-sensitive fluorescent probe 2′, 7′-dichlorofluorescein diacetate ($H_2$-DCFDA) (Molecular Probes Inc., Eugene, OR, USA) at a final concentration of 5 μM for 30 min. The cells were washed and resuspended in PBS, and then ROS amount was measured by flowcytometry.

## Results

### NCH-51 induces apoptosis greater than SAHA

We first evaluated the growth inhibitory effects of NCH-51 on a variety of lymphoid malignant cell lines (Figure 1a). A tentative result in a multiple myeloma cell line U266 cells is shown in Figure 1b. In most of the cell lines including U266 cells, NCH-51 exhibited a stronger growth inhibitory effect than SAHA at 3 μM for 24 h treatment, whereas prolonged incubation for 72 h did not show such a difference. It is noted that there was no significance in the growth inhibitory effect on four healthy donor PBMCs between NCH-51 and SAHA ($IC_{50}$ values of both agents were higher than 30 μM), suggesting a cell-type specific cytotoxicity of NCH-51. We then analyzed the apoptosis and cell cycle distribution after the treatment with NCH-51 or SAHA. In the six cell lines (Jurkat, ED-40515(−), MEC2, U266, XG7 and ILKM-2), all of which showed a high susceptibility to NCH-51 ($IC_{50}$<3 μM), NCH-51 strongly induced apoptosis greater than SAHA after 24 h treatment as demonstrated by generation of sub-$G_1$ cells (Figure 1c and Table 1). In fact, when U266 cells were treated with NCH-51, cleaved forms of caspase-9, -8, -3 and PARP could be detected after 8 h, evidently at 16 h, although no activation of caspase-7 was detected (Figure 1d), suggesting that NCH-51 induces apoptosis through both extrinsic (type I) and intrinsic (type II) pathways[28] in the short-term treatment. On the other hand, cell cycle analysis revealed that NCH-51 increased the cell number at $G_2$/M-phase and reduced the number at $G_1$- or S-phase in most of the cell lines examined (Table 1, right column). No significant difference in the effects on cell cycle regulation was observed between NCH-51- and SAHA-treated cells. These observations suggest that the apoptosis-inducing activity might be attributable to the difference in the observed growth inhibitory effects between NCH-51 and SAHA.

### NCH-51 regulates the expressions of antioxidant molecules at the protein level

To identify the target molecules regulated by NCH-51, we analyzed the RNA and protein expression profiles. cDNA microarray analysis using U266 cells showed that NCH-51 treatment upregulated the expression of *p21* and *p19* (Supplementary Table 1), confirming the previous reports by us[11] and others.[12–14] On the other hand, NCH-51 downregulated the gene expression of *CFLAR* (*c-FLIP*), *survivin* and *BCL2L2* (*bcl-w*), which act as antiapoptotic molecules. These results suggested that these genes were responsible for the growth inhibitory action of NCH-51, however, there was no notable difference in mRNA expression between NCH-51- and SAHA-treated cells. We then performed the proteome analysis. Whole cell extracts were prepared from U266 cells treated with or without NCH-51, and the protein samples were labeled with fluorescent dyes and applied to 2D electrophoresis (Figure 2a). By comparing the amounts of cellular proteins, we identified 14 proteins that varied relatively to NCH-51 treatment (Table 2). Ten proteins including nucleotide diphosphate kinase A (NDPKA), peroxiredoxin 1 and 2 (PRDX1, 2), glutathione *S*-transferase P1-1 (GSTP1-1), 14-3-3 zeta/delta, $Cl^-$ intracellular channel proteins 1 and 4 (CLIC1, 4), proteasome subunit α3, protease activator 28 β subunit and Rho GDI α were upregulated, and four proteins including alanyl-tRNA synthetase (AARS), elongation factor-2 (EF-2), heat-shock 70 kDa protein 8 (HSPA8) and mitochondrial inner membrane protein, were downregulated after the treatment with NCH-51. Interestingly, some of these proteins upregulated by NCH-51 belong to a class of antioxidant molecules. It is noted that PRDX1 and PRDX2 were upregulated at both mRNA and protein levels, thus they are considered to be upregulated at the gene expression level, whereas most of the proteins were upregulated without induction at the gene expression level. In contrast, EF-2 and HSPA8 were downregulated at the protein level. The effects of NCH-51 and SAHA on the expression of EF-2 and PRDX1 were then verified. As shown in Figure 2b, EF-2 protein level was decreased either by NCH-51 or SAHA in the cell lines such as U266, ED-40515 (−) and XG7 cells that were highly susceptible to HDACi. EF-2 was decreased after 16 h treatment with these HDACi (data not shown). On the other hand, in the cell lines such as MEC2, Daudi and KM5 cells that were less sensitive to HDACi, EF-2 protein level was not significantly changed. PRDX1 protein level was upregulated by the treatment with either NCH-51 or SAHA in ED-40515 (−), U266, XG7 and MEC2 cells. SAHA seemed to upregulate PRDX1 more than NCH-51.

**Table 1** The profiles of apoptosis and cell cycle distribution

| *Cell line* | *HDAC inhibitor (μM)* | *Apoptotic cell[a] (%)* | *Cell cycle distribution[a] (%)* | | | |
|---|---|---|---|---|---|---|
| | | | *sub $G_1$* | *$G_1$* | *S* | *$G_2$/M* |
| Jurkat | Untreated control | 6.30 | 5.11 | 50.39 | 20.76 | 20.64 |
| | SAHA | | | | | |
| | 3 μM | 13.45 | 28.56 | 9.15 | 12.97 | 46.22 |
| | 30 μM | 28.97 | 32.39 | 7.06 | 18.10 | 40.83 |
| | NCH-51 | | | | | |
| | 3 μM | 19.27 | 42.66 | 8.05 | 10.04 | 36.28 |
| | 30 μM | 35.45 | 42.69 | 7.64 | 14.41 | 32.21 |
| MT-2 | Untreated control | 6.84 | 3.02 | 63.25 | 15.29 | 15.64 |
| | SAHA | | | | | |
| | 3 μM | 8.23 | 9.41 | 49.04 | 11.70 | 26.36 |
| | 30 μM | 8.75 | 10.35 | 62.95 | 6.15 | 13.96 |
| | NCH-51 | | | | | |
| | 3 μM | 8.45 | 3.26 | 62.21 | 16.34 | 16.53 |
| | 30 μM | 8.62 | 5.38 | 71.64 | 8.35 | 12.22 |
| ED-40515 (−) | Untreated control | 6.44 | 8.40 | 46.82 | 23.30 | 19.67 |
| | SAHA | | | | | |
| | 3 μM | 20.74 | 18.88 | 21.41 | 19.07 | 36.90 |
| | 30 μM | 20.12 | 26.87 | 22.20 | 20.49 | 27.75 |
| | NCH-51 | | | | | |
| | 3 μM | 22.12 | 27.10 | 28.04 | 19.04 | 23.91 |
| | 30 μM | 21.33 | 26.54 | 25.09 | 20.56 | 25.72 |
| MEC2 | Untreated control | 3.20 | 5.66 | 60.06 | 19.96 | 12.16 |
| | SAHA | | | | | |
| | 3 μM | 4.84 | 12.32 | 37.33 | 19.84 | 26.70 |
| | 30 μM | 8.22 | 18.14 | 29.46 | 22.63 | 25.12 |
| | NCH-51 | | | | | |
| | 3 μM | 6.50 | 16.22 | 36.43 | 19.28 | 24.75 |
| | 30 μM | 11.08 | 21.24 | 30.47 | 20.93 | 23.29 |
| MO1043 | Untreated control | 4.14 | 0.89 | 54.88 | 20.75 | 17.87 |
| | SAHA | | | | | |
| | 3 μM | 4.30 | 3.45 | 68.83 | 7.49 | 15.41 |
| | 30 μM | 15.96 | 18.85 | 48.29 | 6.62 | 23.14 |
| | NCH-51 | | | | | |
| | 3 μM | 3.74 | 2.47 | 73.90 | 7.17 | 12.88 |
| | 30 μM | 14.93 | 21.75 | 48.79 | 6.14 | 21.03 |
| Daudi | Untreated control | 1.62 | 1.62 | 52.02 | 22.77 | 19.55 |
| | SAHA | | | | | |
| | 3 μM | 2.08 | 2.17 | 23.65 | 22.33 | 46.30 |
| | 30 μM | 2.12 | 2.34 | 22.83 | 19.75 | 48.21 |
| | NCH-51 | | | | | |
| | 3 μM | 2.64 | 1.90 | 50.38 | 14.74 | 27.71 |
| | 30 μM | 3.04 | 2.19 | 25.68 | 22.19 | 43.28 |
| U266 | Untreated control | 6.17 | 6.30 | 67.42 | 10.99 | 13.02 |
| | SAHA | | | | | |
| | 3 μM | 17.65 | 11.91 | 56.24 | 10.35 | 19.72 |
| | 30 μM | 29.73 | 17.06 | 48.70 | 12.69 | 19.68 |
| | NCH-51 | | | | | |
| | 3 μM | 22.90 | 13.39 | 54.07 | 11.60 | 18.62 |
| | 30 μM | 32.63 | 18.90 | 49.15 | 13.40 | 18.94 |
| XG7 | Untreated control | 7.27 | 7.58 | 49.21 | 20.34 | 23.37 |
| | SAHA | | | | | |
| | 3 μM | 8.74 | 8.50 | 50.40 | 8.33 | 28.32 |
| | 30 μM | 9.43 | 15.38 | 34.23 | 15.10 | 28.21 |
| | NCH-51 | | | | | |
| | 3 μM | 11.47 | 10.00 | 49.32 | 8.62 | 28.62 |
| | 30 μM | 13.13 | 17.87 | 35.44 | 14.67 | 27.93 |
| KM5 | Untreated control | 4.24 | 2.91 | 42.15 | 27.85 | 23.43 |
| | SAHA | | | | | |
| | 3 μM | 4.30 | 6.32 | 31.85 | 31.44 | 26.13 |
| | 30 μM | 15.96 | 23.37 | 20.62 | 26.19 | 24.68 |
| | NCH-51 | | | | | |
| | 3 μM | 3.74 | 6.75 | 38.34 | 29.96 | 20.84 |
| | 30 μM | 18.46 | 20.33 | 27.77 | 23.29 | 24.31 |